HHS Public Access

Author manuscript

Mol Cell. Author manuscript; available in PMC 2023 August 18.

Published in final edited form as:

Mol Cell. 2022 August 18; 82(16): 3089–3102.e7. doi:10.1016/j.molcel.2022.06.033.

S-nitrosylation is required for β_2AR desensitization and experimental asthma

Fabio V. Fonseca[1], **Thomas M. Raffay**[2], **Kunhong Xiao**[3,**], **Precious J. McLaughlin**[1], **Zhaoxia Qian**[1], **Zachary W. Grimmett**[1], **Naoko Adachi**[1,***], **Benlian Wang**[4], **Alfred Hausladen**[1], **Brian A. Cobb**[5], **Rongli Zhang**[6], **Douglas T. Hess**[1], **Benjamin Gaston**[2,****], **Nevin A. Lambert**[7], **James D. Reynolds**[1,8], **Richard T. Premont**[1,8], **Jonathan S. Stamler**[1,8]

[1]Institute for Transformative Molecular Medicine, Case Western Reserve University School of Medicine, Cleveland, OH 44106

[2]Department of Pediatrics, Case Western Reserve University School of Medicine, Cleveland, OH 44106

[3]Department of Medicine, Duke University School of Medicine, Durham, NC 27710

[4]Center for Proteomics and Bioinformatics, Department of Nutrition, Case Western Reserve University School of Medicine, Cleveland, OH 44106

[5]Department of Pathology, Case Western Reserve University School of Medicine, Cleveland, OH 44106

[6]Cardiovascular Research Institute, Case Western Reserve University School of Medicine, Cleveland, OH 44106

[7]Department of Pharmacology and Toxicology, Medical College of Georgia, Augusta University, Augusta, GA 30912

[8]Harrington Discovery Institute, University Hospitals Cleveland Medical Center, Cleveland, OH 44106

Lead contact and corresponding author: Jonathan Stamler, jss156@case.edu.

*present address: Center for Breakthrough Medicines at Discovery Labs, King of Prussia, PA 19406

**present address: Allegheny Health Network Cancer Institute, Pittsburgh, PA 15202

***present address: Biosignal Research Center, Kobe University, Kobe, 657-8501 Japan

****present address: Department of Pediatrics, Indiana University School of Medicine, Bloomington, IN 47405

Author contributions

Conceptualization FVF, JSS; Methodology FVF, TMR, BW, AH, JDR, NAL; Formal analysis FVF, TMR, DTH, NAL, RTP, RJL, JSS; Investigation FVF, TMR, KX, BW, PJM, ZQ, AH, NA, DTH, BAC, NAL, RTP; Writing (original draft) RTP, FVF; Writing (review and editing) TMR, BAC, JDR; Supervision, Project Administration and Funding Acquisition JSS.

Declaration of Interests

JSS has patents relating to nitrosylation, is a founder of SNO bio, and serves as a paid consultant to EFC, which is developing NO-based technology. CWRU and UHCMC have management plans in place. The other authors declare no conflicts.

Supplemental Materials:

Supplemental Figures 1–7

Supplemental Table I

Summary

The β_2-adrenergic receptor (β_2AR), a prototypic G protein-coupled receptor (GPCR), is a powerful driver of bronchorelaxation, but the effectiveness of β-agonist drugs in asthma is limited by desensitization and tachyphylaxis. We find that during activation, the β_2AR is modified by S-nitrosylation, which is essential for both classic desensitization by PKA as well as desensitization of NO-based signaling that mediates bronchorelaxation. Strikingly, S-nitrosylation alone can drive β_2AR internalization in the absence of traditional agonist. Mutant β_2AR refractory to S-nitrosylation (Cys265Ser) exhibits reduced desensitization and internalization, thereby amplifying NO-based signaling, and mice with Cys265Ser mutation are resistant to bronchoconstriction, inflammation, and the development of asthma. S-nitrosylation is thus a central mechanism in β_2AR signaling that may be operative widely among GPCRs and targeted for therapeutic gain.

eTOC blurb

Post-translational modification of the β_2AR by S-nitrosylation, resulting from receptor activation or direct modification, promotes receptor desensitization and caveolar internalization. Preventing β_2AR S-nitrosylation leads to sustained receptor signaling, thereby increasing cAMP, Erk and NO. Mice with mutant β_2AR refractory to S-nitrosylation are resistant to bronchoconstriction, inflammation and development of asthma, suggesting that this newly-identified desensitization mechanism may be targeted therapeutically in obstructive airway diseases.

Graphical Abstract

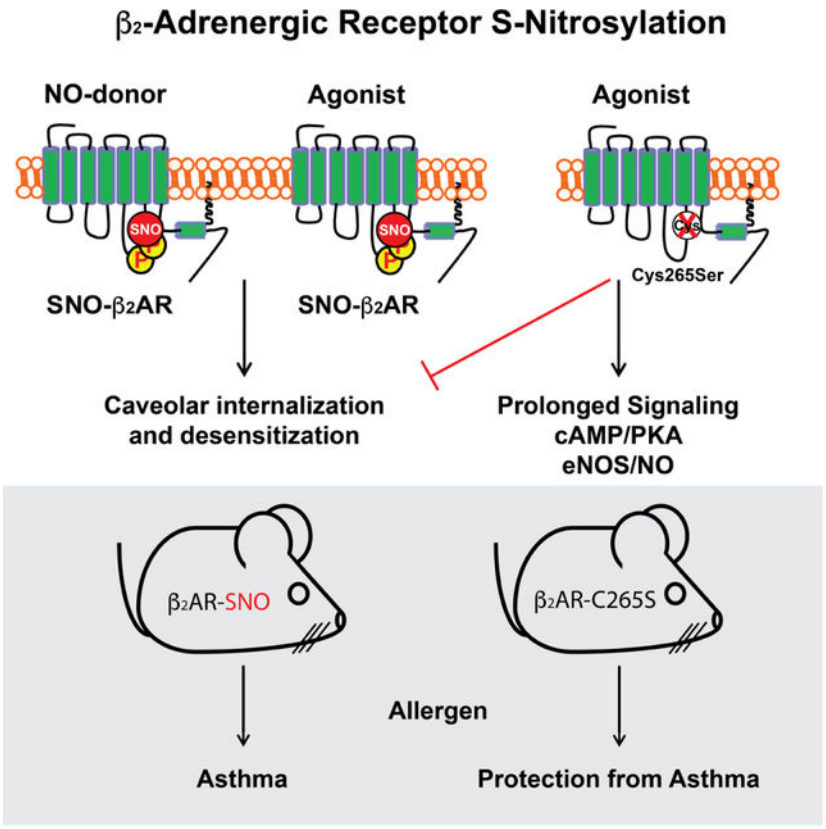

Keywords

S-nitrosylation; asthma; β_2-adrenergic receptor; beta-agonist; nitric oxide; desensitization; receptor internalization; airway hyperreactivity; caveolae

Introduction

Asthma is an allergic lung disease where chronic inflammation leads to airway remodeling and hyperreactivity that reduces lung function (Papi et al., 2018). The β_2-adrenergic receptor (β_2AR) is a G protein-coupled receptor (GPCR) that promotes airway relaxation, and β_2AR agonists find extensive use as asthma therapeutics (Matera et al., 2020; Wendell et al., 2020). However, overstimulation of β_2AR by β-agonists drugs can be detrimental and even lead to death, limiting their utility as front-line therapy (Kersten et al., 2017). Mechanistically, 'overstimulation' results in desensitization and downregulation of the β_2AR (Wendell et al., 2020), serving as a model for GPCR aberrancy in disease. The molecular basis of receptor desensitization in the context of disease is not well understood.

Activation of the β_2AR stimulates production of nitric oxide (NO) (Figueroa et al., 2009), which is implicated in airway relaxation (Antosova et al., 2017). However, the classic NO/guanylyl cyclase/protein kinase G (PKG) pathway that mediates relaxation of vascular smooth muscle has less relevance to airway smooth muscle (Gaston et al., 1994). Additionally, NO directly regulates proteins through S-nitrosylation, the post-translational modification of cysteine residues to form S-nitrosothiols (SNOs) (Hess et al., 2005). Protein S-nitrosylation may involve multienzyme machinery (Jia et al., 2014; Nakamura et al., 2021; Que et al., 2005; Seth et al., 2018; Stomberski et al., 2019) that conjugates and removes NO from proteins, including key GPCR regulatory components (G protein-coupled receptor kinase 2 (GRK2) (Whalen et al., 2007) and β-arrestins 1 and 2 (Hayashi et al., 2018; Ozawa et al., 2008)), which may influence airway responsivity (Que et al., 2005). These data raise the idea that effects of NO/SNO on airway tone may be mediated through regulation of the β_2AR itself.

The β_2AR co-localizes with eNOS (NO synthase type 3) to plasma membrane caveolae (Schwencke et al., 1999; Shaul et al., 1996), and active β_2AR stimulates the production of NO (Figueroa et al., 2009). Further, β_2AR signaling has been reported be inhibited by NO (Abi-Gerges et al., 2002; Adam et al., 1999), but the underlying mechanisms have not been identified. β_2AR has 13 cysteines, including multiple intracellular residues potentially available for S-nitrosylation (Gether et al., 1997a; Wanschel et al., 2014). We therefore reasoned that the β_2AR might be regulated by S-nitrosylation to desensitize the receptor, and demonstrate that β_2AR stimulation is in fact coupled to S-nitrosylation of three intracellular Cys residues, including one (C265) that serves in allosteric control of receptor signaling, desensitization and internalization. Mutant mice refractory to S-nitrosylation are profoundly resistant to developing asthma. Our findings reveal general receptor signaling principles, including previously unappreciated roles for NO/SNO in receptor signaling, trafficking and desensitization. They also uncover a major role for NO/SNO in relaxation of airways that

has been overlooked and expound a paradigm for how β_2AR function might be targeted in asthma or other obstructive airway disease.

Results

β_2AR is S-nitrosylated during activation

Treatment of HEK293 cells with the cell-permeable SNO donor ethyl ester CysNO (ECNO) promoted the S-nitrosylation of human β_2AR (Figure 1A). As measures of specificity of S-nitrosylation in the SNO-RAC assay (Forrester et al., 2009), no SNO signal was generated in the absence of ascorbate (control) or when SNO is removed by UV photolysis prior to assay (Foster and Stamler, 2004). Importantly, activation of the β_2AR with isoproterenol (ISO) also increased SNO-β_2AR, through the activity of eNOS native to HEK293 cells (Hayashi et al., 2018; Ozawa et al., 2008), since pretreatment with the NOS inhibitor L-NMMA eliminated the agonist-stimulated SNO-β_2AR signal (Figure 1B). ISO-stimulated SNO-β_2AR was maximal after 10 minutes (Supplemental Figure 1A), and multiple β_2AR agonists and partial agonists promoted SNO-modification of the receptor (Supplemental Figure 1B). We used mass spectrometry to identify sites on the β_2AR modified by SNO after ECNO treatment and identified peptides containing three distinct sites: Cys265, Cys341 and Cys378 (Supplemental Figure 1C,D). Mutations in the β_2AR of all Cys residues in the carboxyl tail region (Cys 328, 341, 378 and 406) plus Cys265 in the third loop near TM6 (five sites), or of the three sites from mass spectrometry (Cys265, Cys341 and Cys378), reduced ISO-stimulated SNO-β_2AR to background levels (Figure 1C, Supplemental Figure 1E,F). Mutation of just one residue, Cys265, dramatically reduced ISO-stimulated SNO-β_2AR (Figure 1D) without affecting expression level (Supplemental Figure 1G,H), establishing this as the primary site of modification. S-nitrosylation of native β_2AR was also detected in mouse lungs (as will be described below) and in human and mouse heart samples (Figure 1 E,F), and the SNO level was increased in ischemic heart failure (Figure 1E) or by ISO infusion in vivo (Figure 1F). In the same human heart samples, SNO-β_1AR was detected in normal heart, and SNO levels increased in both ischemic and non-ischemic heart failure (Supplemental Figure 1I). Additionally, angiotensin II receptor 1 (ATR1) was also S-nitrosylated basally in HEK cells, and this level was increased by AngII treatment (Supplemental Figure 1J). Thus, multiple GPCRs are S-nitrosylated following agonist stimulation or disease, and β_2AR is modified by eNOS-derived SNO, primarily at Cys265, in both model cells and in vivo. Altogether, these data suggest a widespread role for S-nitrosylation in normal GPCR function in health and disease.

β_2AR S-nitrosylation at Cys265 regulates receptor signaling

The β_2AR signals through cAMP (via G_s) and Erk (via G_i/β-arrestin), but also through activation of eNOS (Queen and Ferro, 2006). To understand the importance of Cys265 modification by SNO in β_2AR function, we assessed signaling by C265 mutant β_2ARs. While ISO-stimulated cAMP accumulation at 10 min of stimulation appeared normal (Supplemental Figure 2A,B), cAMP signaling by C265S (and C265A) mutants remained elevated through 30 min (Supplemental Figure 2C). On further analysis, cAMP accumulation by C265S β_2AR remained markedly elevated through 5 hours (Figure 1G). Consistent with this, a pan-PKA-substrate phospho-site antibody detected prolonged

elevation of PKA substrate phosphorylation following activation of C265S β_2AR versus transient response of WT receptor (Supplemental Figure 2D). Similarly, Erk activation was prolonged after ISO-stimulation of C265S (and C265A) mutant receptors (Figure 1H, Supplemental Figure 2E). Using pertussis toxin (PTX), which prevents receptor activation of G_i pathways, we determined that ~80% of Erk activation by mutants was dependent on G_i proteins, in contrast to the much lower (~30–40%) G_i-dependence of WT receptor (reflecting WT dependence on βarrestin) (Lefkowitz et al., 2002) (Supplemental Figure 2E,F). Also, ISO-stimulated cellular S-nitrosylation was elevated in cells expressing C265S β_2AR, demonstrating increased β_2AR signaling through G_i to eNOS/NO that is sensitive to PTX (Figure 1I, Supplemental Figure 2G). This increased cAMP accumulation was not due to reduced phosphodiesterase, as basal PDE activity was higher in C265S-expressing cells (Supplemental Figure 2H). Altogether, these data demonstrate that S-nitrosylation of β_2AR at Cys265 is important for termination of receptor signaling to PKA, Erk and eNOS. Furthermore, the sustained production of cAMP suggests that classic PKA phosphorylation of the β_2AR is not sufficient to promote desensitization.

β_2AR S-nitrosylation regulates receptor internalization through a PKA-caveolae pathway

Sustained signaling by Cys265-mutant β_2ARs suggested that S-nitrosylation at Cys265 enables desensitization and/or trafficking from the cell surface. ISO-stimulated internalization of β_2AR-C265A mutant from the cell surface was impaired (Figure 2A). Agonist-activated β_2AR is reported to be internalized in clathrin-coated pits primarily through a pathway dependent on receptor phosphorylation by GRKs and binding to β-arrestins that scaffold adaptin-AP2 and clathrin (Ferguson et al., 1996; Laporte et al., 1999; Zhang et al., 1996). When β_2AR C265A mutant was stimulated by ISO, receptors moved into intracellular vesicles and also recruited β-Arrestin2-GFP to the plasma membrane (Figure 2B, Supplemental Figure 3A), indicating that the mutation did not prevent agonist-activated β-Arrestin2 recruitment or the receptor phosphorylation that this requires.

Surprisingly, the NO-donor ECNO (or NO derived from eNOS) promoted internalization of WT β_2AR from the cell surface in the absence of agonist, and this internalization was absent in the 5-cysteine or C265A mutants (Figure 2C,D). Dual labeling of β_2AR and β-Arrestin2 showed that, in contrast to ISO stimulation, ECNO-driven receptor internalization did not lead to association of β-Arrestin2 with β_2AR (Figure 2E). ECNO treatment was unable to recruit β-Arrestin2-GFP to β_2AR at the plasma membrane or intracellular vesicles (Figure 2F), suggesting that NO/SNO induces an alternative pathway for β_2AR internalization. To investigate this matter more rigorously, we used double-knockout (DKO) MEF cells lacking β-Arrestin1 and β-Arrestin2 (Kohout et al., 2001) to measure β_2AR internalization, and found that these cells lacking β-Arrestins effectively internalized β_2AR after stimulation with ECNO or ISO. Thus, S-nitrosylation-dependent receptor internalization does not require β-Arrestins (Supplemental Figure 3B). To confirm a role for endogenously derived NO in β-Arrestin-independent internalization, we expressed exogenous eNOS in these cells. Notably, eNOS induced receptor removal from the cell surface (Supplemental Figure 3B). Furthermore, the NOS inhibitor L-NMMA inhibited ISO-stimulated β_2AR internalization (Supplemental Figure 3C). Taken together, these data demonstrate that endogenous NOS and NO can regulate β_2AR internalization independently of β-Arrestins.

Because β-Arrestin2 recruitment to β_2AR requires receptor phosphorylation by GRKs, we examined a β_2AR mutant that lacks GRK phosphorylation sites (GRK$^-$ mutant) (Seibold et al., 1998). ECNO treatment stimulated equivalent internalization of the WT and GRK$^-$ β_2AR (Supplemental Figure 3D). In contrast to the β_2AR, the ISO-stimulated β_1AR is known to internalize through two distinct pathways, a PKA/caveolae pathway as well as the GRK/β-arrestin/clathrin pathway (Rapacciuolo et al., 2003). Since β_2AR localizes in caveolae in cell types that have these domains (Ostrom and Insel, 2004; Xiang et al., 2002) we sought to determine if ECNO-treated β_2AR might also utilize a caveolae pathway. Indeed, ECNO-induced internalization of both WT and GRK$^-$ β_2AR were inhibited equally by pretreatment with the caveolae inhibitors β-methyl-D-cyclodextrin (βMCD), genistein (Gen) or filipin III (Fili) (Supplemental Figure 3D,E.F). ECNO-stimulated internalization of the PKA$^-$ mutant β_2AR, which lacks the four consensus PKA phosphorylation sites (Friedman et al., 2002), was greatly diminished, and was unaffected by treatment with chlorpromazine (Chl), an inhibitor of the clathrin internalization pathway (Figure 2G), while ECNO-stimulated internalization of both WT and GRK$^-$ mutant β_2AR were both blocked by the PKA inhibitor H-89 (Figure 2H). Taken together, these data indicate that NO stimulates β_2AR internalization through a caveolae pathway and that PKA phosphorylation of the receptor is required for NO-stimulated transit through caveolae.

Inhibition of the GRK/β-arrestin/clathrin pathway using the GRK$^-$ mutant β_2AR renders ISO-stimulated GRK$^-$ β_2AR internalization sensitive to the caveolae inhibitors βMCD, Gen and Fili (Supplemental Figure 3G,H,I). In the same way, inhibition of the caveolae pathway using the PKA$^-$ mutant β_2AR renders ISO-stimulated receptor internalization sensitive to the clathrin inhibitor Chl (Supplemental Figure 3J), while inhibition of PKA using the inhibitor H-89 reduces internalization of the WT β_2AR but ablates internalization of the GRK$^-$ mutant β_2AR (Figure 2I). Altogether, these data show that S-nitrosylation at Cys265 drives β_2AR internalization through a PKA-caveolae pathway, even in the absence of a receptor agonist, and mutation of Cys265 to prevent this modification reduces receptor internalization from the cell surface to prolong signaling activity. Thus, S-nitrosylation of Cys265 is necessary and sufficient (absent agonist) for receptor internalization via caveolae.

β_2AR S-nitrosylation and PKA-phosphorylation are interdependent

Notably, removal of PKA phosphorylation sites from β_2AR significantly reduced the ability of ECNO to S-nitrosylate the receptor (Figure 3A). Moreover, ISO-stimulated S-nitrosylation of WT β_2AR was inhibited by treatment with the PKA inhibitor H-89 or KT-5720, or with the G_i inhibitor PTX that uncouples receptor from eNOS (Figure 3B, Supplemental Figure 4A). Thus remarkably, S-nitrosylation of β_2AR is dependent on its phosphorylation by PKA. PKA phosphorylates two pairs of serines on the β_2AR, at Ser261/262 in the third intracellular loop adjacent to the Cys265 SNO site and at Ser345/346 in the carboxyl terminal tail (Hausdorff et al., 1989), and PKA phosphorylation at Ser261/262 enables β_2AR activation of G_i proteins (Daaka et al., 1997). ECNO-treatment induces significant phosphorylation of WT β_2AR at Ser261/262, but phosphorylation is reduced in the C265A mutant receptor (Figure 3C). ECNO or ISO do not stimulate phosphorylation at Ser345/346 over basal on the WT receptor, but phosphorylation levels with or without stimulation are significantly reduced in the C265A mutant receptor

(Supplemental Figure 4B). Thus, β_2AR phosphorylation by PKA is dependent on S-nitrosylation of Cys265.

ECNO-mediated PKA phosphorylation of WT β_2AR in the absence of ISO (Figure 3D) suggests a G protein-independent activity. Interestingly, PKA is directly activated by S-nitrosylation (Burgoyne and Eaton, 2009), so we tested whether SNO-PKA, rather than the traditional cAMP pathway, might mediate β_2AR phosphorylation. ECNO treatment led to increased phospho-β_2AR at Ser261/262 and Ser345/346 that was not reduced by pretreatment with adenylyl cyclase inhibitors (Figure 3D, Supplemental Figure 4C,D), suggesting that NO activates PKA independently of β_2AR activation. Altogether, these data show that Cys265 S-nitrosylation is critical for PKA activation by the β_2AR leading to phosphorylation of the receptor.

Since PKA phosphorylation of β_2AR at Ser261/262 is known to be necessary for β_2AR switching its coupling from G_s to G_i (Daaka et al., 1997), we wondered if G protein coupling was altered by β_2AR S-nitrosylation. Using BRET-based assays for G_s and G_i coupling to the β_2AR, we found no differences of C265A or C265S mutant receptors compared to WT β_2AR (Supplemental Figure 4E), indicating that SNO-β_2AR likely does not alter G protein coupling directly.

Overall, our results suggest a model for β_2AR function (Supplemental Figure 4F) where β_2AR stimulation promotes G_s-PKA activation that phosphorylates the receptor to promote G_i coupling and activation of eNOS, leading to feedback S-nitrosylation of the receptor. Receptor S-nitrosylation and PKA phosphorylation together induce trafficking of the receptor through caveolae, distinct from the GRK/arrestin/clathrin-mediated internalization expected for β_2AR. β_2AR S-nitrosylation in the absence of receptor activation by agonist promotes agonist-independent receptor phosphorylation by PKA and internalization through the caveolae pathway. In the absence of β_2AR S-nitrosylation (due to NOS inhibition, G_i or PKA inhibition, or to PKA-site or SNO-site mutations), the agonist-activated receptor fails to internalize through this caveolae pathway, leading to prolonged signaling by G_s-cAMP/PKA, and also by G_i-eNOS/NO. Prolonged signaling by G_s and G_i in mutant receptors suggests that in the wildtype β_2AR, S-nitrosylation functions as a feedback regulatory mechanism to desensitize the receptor to G_i-eNOS signaling, in coordination with traditional feedback desensitization through G_s-PKA signaling.

β_2AR S-nitrosylation masks NO-based bronchodilation in vivo

β_2AR is expressed in the lung, and native β_2AR in mouse lung is S-nitrosylated under basal conditions (Figure 4A, Supplemental Figure 1J). To understand the role of β_2AR S-nitrosylation in vivo, we generated knock-in mice bearing the β_2AR C265S mutation (Supplemental Figure 5A,B,C). *ADRB2*$^{C265S/C265S}$ (C265S) mice survive and breed normally, and have normal level of expression of β_2AR in the lung (Supplemental Figure 5D,E). When subjected to airway challenge with methacholine, a muscarinic agonist that constricts airways, C265S mice are substantially protected from airway constriction (Figure 4B). We predicted that this airway protection by the C265S β_2AR would be dependent on prolonged PTX-sensitive G_i signaling to eNOS, and pretreatment of mice with PTX eliminated the protective effect of C265S on methacholine-induced airway resistance (PTX

also exacerbated airway constriction in WT mice) (Figure 4C). Further, inhibition of NOS, either pharmacologically with L-NAME or genetically by crossing with mice deficient in eNOS ($eNOS^{-/-}$), eliminated the protective effect of C265S on methacholine-induced airway constriction (Figure 4C). Taken together, these data demonstrate a major, previously unappreciated role for NO in β_2AR-mediated airway relaxation. However, this G_i-stimulated eNOS-mediated airway relaxation is masked by feedback S-nitrosylation of the β_2AR.

To extend these findings to other physiological systems, we assessed contraction and relaxation of isolated aorta in vitro. Contraction in response to phenylephrine (through Gq-coupled α_1-adrenergic receptor) is markedly reduced in C265S mice, while ISO-stimulated relaxation is essentially unchanged (Supplemental Figure 5F,G).

β_2AR S-nitrosylation promotes asthmatic response

Airway hyperreactivity is one hallmark of asthma, so we reasoned that C265S mice might be protected from hyper-reactivity in an asthma model. We sensitized mice to house dust mite allergens (*Dermatophagoides pteronyssinus*, D.p. or *Dermatophagoides farina*, D.f.), and tested the sensitivity of airways to bronchoconstriction by methacholine. While WT mice exhibited increased methacholine-induced airway resistance after exposure to D.p. or D.f. allergens, C265S mice exhibited minimal airway bronchoconstriction to methacholine, with or without allergen pre-exposure (Figure 5A,B). Cyclic AMP levels in lung homogenates of naive mice were elevated in C265S vs WT, replicating cellular data (Figure 1G), and remained high after allergen exposure (Figure 5C), consistent with blocked desensitization. Lung expression of muscarinic receptors as assessed by qRT-PCR, and M1, M2, M3 and M5 receptor mRNA levels failed to increase after allergen sensitization of C265S β_2AR mice (Supplemental Figure 6A–D). Other muscarinic pathway components (Cpi17, RhoA, Prkcd) showed a similar pattern, while CD38 expression dropped in allergen-treated C265S β_2AR samples (Supplemental Figure 6E–H). Thus, the protective effect of C265S β_2AR expression appears to result from both direct signaling effects (chronically elevated cAMP and NO) and beneficial compensatory changes (reduction of muscarinic signaling components that lead to bronchoconstriction). Understanding of this well-described cross-talk between muscarinic and adrenergic systems is poor, but evidently may reflect S-nitrosylation status of β_2AR based on evidence in C265A mice.

Asthma is characterized by elevated cytokines and immune cell infiltration into the lung and these have been linked to β_2AR activity and cAMP (Papi et al., 2018; Wendell et al., 2020). Asthma-associated inflammatory cytokines, including IL4, IL5, IL9, IL10, IL13 and interferon-γ, all failed to increase after allergen exposure in C265S mouse lungs (Supplemental Figure 7A–F). Quantification of infiltrated immune cells from bronchoalveolar lavage fluid following allergen exposure revealed that expected increases in total white blood cells, neutrophils, lymphocytes, and eosinophils are all blunted in C265S mice (Figure 6A–D). Chronic inflammation in asthma leads to airway remodeling, where lung structure is altered by immune- and injury-driven proliferation of smooth muscle, epithelia, fibroblasts and extracellular matrix to generate thicker airway walls and narrowed airway lumen (Papi et al., 2018; Wendell et al., 2020). Lungs from allergen-treated C265S mice failed to show elevated levels of epithelial cell adhesion molecule (EpCAM)

or immune cell marker myeloperoxidase (MPO) (Figure 6E). Lung sections stained with Masson's Trichrome revealed thickened airway walls with fibrosis in allergen-sensitized WT mice, but C265S mice were largely protected from these changes (Figure 6F). When lung sections were stained with H&E, thickened airways and focal inflammation within alveoli that were evident in allergen-sensitized WT mice were notably absent from treated C265S mice (Figure 6G). Altogether, these data demonstrate that S-nitrosylation of the β_2AR at Cys265 subsequent to its activation, or through heterologous production of NO, is a critical part of classic desensitization of this receptor, and in an asthma model in vivo, this receptor downregulation is ultimately maladaptive and contributes to multiple aspects of allergic asthma pathology.

Discussion

The classic GPCR signaling paradigm entails activation of G protein, synthesis of cAMP, and PKA-driven phosphorylation events, including desensitization and internalization of the receptor. For airway β_2AR, transduction results in cAMP/PKA-mediated relaxation of airway smooth muscle, providing a mainstay treatment for airway diseases. In this report, we show that prototypic signaling through the β_2AR involves an essential, previously unappreciated role for nitric oxide. Notably, S-nitrosylation by NO is required for both classic desensitization by PKA as well as desensitization of previously unappreciated NO-based signaling that mediates airway relaxation. Mutant receptor (C265S) resistant to S-nitrosylation cannot be desensitized and thus maintains signaling to cAMP/PKA, but also to eNOS/NO necessary for airway relaxation. Mice bearing the β_2AR-C265S mutation thus lose the ability to bronchoconstrict, leading to marked protection from asthma. We conclude that β_2AR S-nitrosylation is a central regulatory mechanism that limits receptor signaling and contributes to the asthmatic phenotype, and that targeting this mechanism to extend β_2AR activity can ameliorate airway disease.

The β_2AR is modified by S-nitrosylation in response to agonists and exogenous sources of NO and exhibits endogenous S-nitrosylation in situ. The major SNO site, Cys265, is located in the receptor third intracellular loop at transmembrane span 6 (TM6), a region critically important for active state conformation changes that mediate G protein coupling (Gether et al., 1997a; Gether et al., 1997b; Kobilka, 2002) and adjacent to one of two clusters of PKA phosphorylation sites (Ser261,262) (Hausdorff et al., 1989). Indeed, Cys265 is commonly used to label β_2AR for conformation measurements relating to TM6 (Gether et al., 1997b; Kobilka, 2002). Additionally, Cys265 is a site for dynamic β_2AR palmitoylation, although on a distinctly slower timescale (hours) and without obvious effects (Adachi et al., 2016). Thus, a regulatory role for Cys265 has not been previously considered. Strikingly evident in our assays is that receptor S-nitrosylation can act as an allosteric promoter of receptor internalization in the absence of orthosteric ligand. This form of receptor regulation has not been described previously and suggests fundamentally distinct approaches to regulate GPCR function. A recent report that thiol alkylators can modify the P2Y6 receptor to drive its internalization and ubiquitin-mediated downregulation (Nishiyama et al., 2022) reinforces our contention that endogenous nitrosylation, as shown here for multiple GPCRs (Figure 1E,F; Figure 4A, Supplemental Figure 1I,J), may represent a general mode of receptor regulation. Inasmuch as signaling by GPCRs may occur within endosomes (Irannejad et

al., 2013), the signaling dynamics of receptors internalized allosterically should be further explored.

Our studies with β_2AR-C265S mutant, and with receptor mutants unable to be phosphorylated by PKA (PKA$^-$), or by GRKs (GRK$^-$) to engage the GRK/arrestin/clathrin internalization pathway, reveal that SNO-β_2AR can unexpectedly engage a distinct PKA/caveolae internalization pathway that has been described for other GPCRs, including the β_1AR (Rapacciuolo et al., 2003), but has not been appreciated previously for β_2AR. That is, in cells where β_2AR activates eNOS, distinct caveolae and clathrin internalization pathways are dynamically engaged in response to feedback regulation by NO or GRKs, respectively. In the β_2AR-C265S mutant or PKA$^-$ mutant, the inability to be S-nitrosylated or PKA phosphorylated thus allows sustained signaling to G_s/cAMP/PKA and β-Arrestin2/Erk, but critically also to G_i/eNOS/NO. However, while signaling to cAMP may be self-limiting given the multiple mechanisms capable of diminishing β_2AR responsiveness over time (e.g. cAMP phosphodiesterases, PKA desensitization of G_s and adenylyl cyclase), sustained NO production via eNOS is independent of cAMP/PKA. That distinct G_s/cAMP/PKA and G_i/eNOS/NO pathways are operative is most clearly evident in β_2AR C265S mice where elevations are seen in both cAMP and NO bioactivity (due to prolonged G_s/G_i signaling) but where protection from bronchoconstriction is abolished by PTX or eNOS inhibition. NO mediated receptor S-nitrosylation is thus a previously unappreciated regulatory mechanism that proceeds from receptor activation and feeds back to desensitize a critical pathway leading to NO production. Ligands (long and short acting β_2-agonists) that bias internalization to one pathway over another or that differentially couple β_2AR to eNOS and thus to receptor S-nitrosylation might be exploited for therapeutic benefit.

β_2AR-C265S mice are not only protected from bronchoconstriction, but also from airway inflammation, consistent with a known role for the β_2AR in asthmatic airway inflammation (Nguyen et al., 2009), and implicating β_2AR S-nitrosylation in the phlogistic effect of β_2AR stimulation. This is a provocative finding, since prolonged or repeated use of β_2AR agonists in asthma has been associated with poor outcomes (including death) in patients and in animal models (Amrani and Bradding, 2017; Knight et al., 2015; Lin et al., 2012; Vitale et al., 2017) and NO derived from inflammatory cells is markedly elevated in asthma (Kharitonov et al., 1994). Further, in mouse models the development of asthma actually requires epinephrine/β_2AR stimulation, and asthma development can be attenuated with β-blockers, which prevent receptor desensitization (Nguyen et al., 2017; Nguyen et al., 2009; Thanawala et al., 2013; Thanawala et al., 2015). Importantly, C265S mutant mice resistant to desensitization are resistant to the development of allergic asthma, including airway hyper-reactivity, immune inflammation and chronic remodeling of the lung.

NO bioactivity plays multiple roles in lung function (Antosova et al., 2017), but there has been little clarity as to its role in asthma. Asthmatics have elevated iNOS activity in immune cells (Kharitonov et al., 1994), and elevated NO gas in exhaled air is used as a biomarker of lung inflammation (Hoyte et al., 2018). However, iNOS knockout mice are not protected from asthma (Landgraf et al., 2005). Likewise, NO can relax airways (Antosova et al., 2017), but eNOS knockouts have no asthmatic phenotype (Mathrani et al., 2007). Thus, the prevailing view is that NO plays a minor role in asthma. Our

data suggest otherwise and provide a fresh perspective whereby signaling through the β_2AR includes a major role for NO/SNO in relaxing airways that is blocked upon β_2AR desensitization. In this model, desensitization of the β_2AR involves an essential role for feedback S-nitrosylation that mediates airway constriction and inflammation in asthmatic mice. Thus, desensitization of the β_2AR is causal in asthma and may likely involve SNOs that can both bronchodilate and S-nitrosylate the receptor. Our data are consistent with reports that endogenous SNOs are potent relaxants in human airways (Gaston et al., 1993) and that the SNO-metabolizing enzyme GSNO reductase (GSNOR) regulates β_2AR signaling and desensitization (Que et al., 2005). Intriguingly, gene association studies have identified β_2AR (*ADRB2*) and GSNOR (*ADH5*) gene polymorphisms in asthma patients (Choudhry et al., 2010; Moore et al., 2009; Wu et al., 2007), and *ADRB2/ADH5* interaction predicts response to β-agonists (Moore et al., 2009), suggesting a mechanistic link involving β_2AR S-nitrosylation. Collectively, these data suggest reevaluation of the role of NO in asthma and an additional therapeutic approach to airway disease.

Limitations of the Study.

Although we identified three sites in the β_2AR that can be S-nitrosylated in model cells, we characterized only the primary site, Cys265. The effect of S-nitrosylation of the other two sites individually and collectively remains unknown, as do conditions that may favor their modification (O'Dowd et al., 1989). Distinct pathways, such as regulation of PP2-dependent β_2AR dephosphorylation that alters receptor re-sensitization, can also lead to asthma protection (Gupta et al., 2015), but whether and how this intersects with β_2AR regulation by SNO (or particularly receptor de-nitrosylation) remain unexamined. The β_2AR has been reported to signal in endosomes after clathrin pathway internalization (Irannejad et al., 2013), but any β_2AR endosomal signaling after caveolar internalization or after β_2AR S-nitrosylation remains undefined. The β_2AR C265S mouse is a constitutive knock-in, so that prolonged or otherwise altered signaling by the mutant receptor through development may lead to adaptive changes. Among the changes we do see are altered expression of multiple signaling proteins in pro-contractile pathways, but the mechanisms linking β_2AR S-nitrosylation and these changes remain uncharacterized. We utilized a mouse model of allergic asthma, which may differ from asthma in humans and other mouse species, and treatment of mice with PTX or L-NAME will have effects outside airways.

STAR Methods

RESOURCE AVAILABILITY

Lead contact—Further information and requests for resources and reagents should be directed to and will be fulfilled by the Lead Contact, Jonathan Stamler (jss156@case.edu).

Materials Availability—Plasmids and animal models generated in this study will be shared by the lead contact upon request, subject to an institutional MTA.

Data and code availability

- Raw image data for all Figures have been deposited with Mendeley and are publicly available as of the date of publication. The accession number is listed in the Key Resources table.
- This paper does not report original code.
- Any additional information required to reanalyze the data reported in this paper is available from the lead contact upon request.

EXPERIMENTAL MODEL AND SUBJECT DETAILS

Animals—Mice with *Adrb2* gene bearing C265S mutation were prepared by homologous recombination by InGenious Targeting Laboratories (Ronkonkoma, NY) (see Supplemental Figure 5A). A 9.3kb gene fragment was subcloned from a mouse C57BL/6 BAC clone (RP23:376J14, H1H), and an FRT/loxP-flanked NEO selection marker gene was inserted downstream of the coding region. The C265S mutation was created by overlap PCR, and this 1.9kb fragment was inserted into the targeting construct using ClaI and MfeI restriction enzymes. G418-resistant C57BL/6 ES cell clones were verified by PCR, Southern blot (see Supplemental Figure 5B), DNA sequencing, and karyotyping before injection into mouse Balb/c blastocysts. Chimeric founder mice were bred to C57BL/6J mice for stable transmission, and the resulting heterozygote mice were bred to the Flp-deleter strain (on C57BL/6J background) to remove the NEO cassette. Heterozygote $Abrb2^{+/C265S}$ mice were interbred to obtain wildtype (WT) and $Adrb2^{C265S/C265S}$ (C265S) mice on the C57BL/6J background for study. Male mice from 2 to 4 months of age were tested in all experiments. Mice were genotyped by PCR from tail-tip genomic DNA using the primers ADRB2-NDEL1: 5'-CCTGACTCACGGAAACAGAGTTATGGG and ADRB2-NDEL2 5'-GGGGAAGCCTGGTTTACACAGAAG (see Supplemental Table I), yielding a 372bp product from the WT allele and a 552bp product from the mutated allele (see Supplemental Figure 5C).

For some experiments, C265S mice were bred with $eNOS^{-/-}$ mice on the C57BL/6J background (Jax) to generate double homozygotes, and $Adrb2^{-/-}$ mice (Jax) were used for tissue harvest.

All animal work was performed under protocols approved by the CWRU IACUC and conformed to standards in the *Guide for the Care and Use of Laboratory Animals*.

Cell lines and culture—The HEK293 stable cell line expressing Flag-β_2AR (W9) was obtained from Robert Lefkowitz, and wildtype HEK293 cells were from ATCC (Manassas, Virginia). HEK293 cells were maintained in high-glucose DMEM media (Life Technologies) with 10% fetal bovine serum and antibiotics at 37°C under 5% CO_2 in a humidified, water-jacketed incubator. HEK293 cells were transfected with plasmid DNAs using the X-tremeGENE 9 transfection reagent (Roche); for stable transfection, cells were subsequently selected for growth in 400 μg/ml G418 (Life Technologies). Cells were serum-starved with DMEM media for 1h prior to treatment with ISO (10 μM for 5 min), ECNO

(100 μM for 10 min), and in some assays, cells were pretreated with PTX (100 ng/ml) for 18h or with inhibitors as described for each assay.

Mouse embryonic fibroblast (MEF) cell lines from β-Arrestin1/β-Arrestin2 double-knockout mice and from control WT mice were obtained from Robert Lefkowitz (Duke University). MEFs were maintained in MEM media (Life Technologies) with 10% fetal bovine serum and antibiotics at 37°C under 5% CO_2 in a humidified, water-jacketed incubator. MEFs were transfected with Flag-β_2AR using X-tremeGENE HP transfection reagent (Roche).

Human tissue—Deidentified human ventricular tissue samples from normal and heart failure patients were obtained from the Duke University Biorepository and Precision Pathology Center (Durham, NC). Because these tissues were exempted from requiring a human studies protocol by the University Hospitals Cleveland Medical Center IRB (Exemption EM-15-35), no PHI (including age or sex) was provided with the tissue samples, only disease status.

METHOD DETAILS

Plasmids and mutagenesis—β-Arrestin2-GFP, Flag-β-Arrestin2, Flag- and HA-tagged human ATR1 and Flag- and HA-tagged human β_2ARs, and PKA^- and GRK^- phosphorylation-site mutant β_2ARs were the kind gift of Robert Lefkowitz (Duke University). Flag-tagged β_2AR mutants were created using the QuikChange II site-directed mutagenesis kit (Agilent), using specific primers (see Supplemental Table I). The split-fluor Gβγ (Venus 156-239-Gβ1, Venus 1-155-Gγ2) and β_2AR-NanoLuc plasmids have been described previously (Masuho et al., 2015; Okashah et al., 2019).

SNO-RAC assay and western blotting—SNO-protein resin-assisted capture (SNO-RAC) was performed as described previously (Forrester et al., 2009). Briefly, frozen cell pellets were lysed in HEN buffer (20mM HEPES, 1mM EDTA, 0.1 mM Neocuproine,) with protease inhibitors (Roche) by sonication, and incubated with the free-sulfhydryl blocking agent S-methyl methanethiosulfonate (MMTS, 0.1%, Sigma). Proteins were washed free of MMTS by repeated acetone precipitation, and SNO removed from proteins by addition of 30 mM ascorbate in HEN buffer (or left on proteins by omitting ascorbate, as a negative control). All manipulations through the ascorbate step were performed in the dark in opaque tubes to minimize light exposure that can remove SNO from proteins, except in experiments where lysates in MMTS were exposed to UV light to remove SNO by photolysis (by incubating lysate in a glass vial on a Stratalinker (Stratagene) for 5 min). Samples were mixed with thiopropyl-Sepharose beads (GE Cytiva) to capture free thiols (sites previously bound to SNO that were freed by ascorbate), and the beads extensively washed. For western blotting identification, bead-bound proteins were eluted and separated by SDS-PAGE on 10% acrylamide gels (Criterion, Bio Rad, Hercules, CA), and detected with anti-tag (Flag or HA) or anti-target antibodies (see Key Resources).

For proteomic analysis, ECNO-treated HEK293 cells were lysed and fractionated into cytosolic and membrane fractions, and the membrane fraction was processed for SNO-RAC, with simultaneous MMTS blocking and membrane extraction with SDS detergent. SNO-RAC beads were digested with trypsin and washed, and bound peptides eluted and

cleaned using C18 Ziptip prior to Orbitrap LC/MS/MS at the CWRU proteomic core facility. Peptides were identified by MASCOT search against the NCBI human NR database.

For standard western blotting of cell lysates and mouse tissues, lysates were prepared in RIPA buffer (Sigma) supplemented with protease inhibitors (Roche). Lysate proteins were quantified using BCA (Bio Rad) and separated by SDS-PAGE on 10% acrylamide gels (Criterion, Bio Rad, Hercules, CA) for detection with anti-tag (Flag or HA) or anti-target antibodies (see Key Resources). For immunoblot detection, transferred nitrocellulose filters were blocked with LI-COR blocking buffer, exposed sequentially to primary and Alexafluor-labeled secondary antisera, and detected on a LI-COR Odyssey imager.

Measurement of cAMP, Phosphodiesterase, Protein kinase A and Erk1/2 activity—PARAMETER mouse/rat cAMP ELISA kit (R&D Systems) was used to measure cAMP accumulation in cell lysates, according to the manufacturer's instructions. cAMP was measured in live cells using HEK293 cells transiently expressing the CAMYEL cAMP BRET biosensor, as described (Jiang et al., 2007), after transfection with Flag-β_2AR, and was also measured in live cells using HEK293 cells stably expressing the luciferase-based cAMP biosensor GloSensor-20F (Fan et al., 2008) (Promega), which were transfected with Flag-β_2AR, then split the next day onto a 96-well plate at 80,000 cells/well. One day later, cells were treated with the GloSensor reagent [Promega; 4% (v/v)] at room temperature for 2 h (and with any inhibitors, as indicated in appropriate figure legends) prior to stimulation with ISO at various doses for 5 min, and cAMP quantified using a NOVOstar microplate reader (BMG Labtech) or a GloMax plate reader (Promega).

cAMP Phosphodiesterase activity was quantified using the Fluorometric cAMP phosphodiesterase activity kit according to the manufacturer's protocol (Biovision, Milpitas, CA) and read on a GloMax plate reader (Promega).

ISO-stimulated phosphorylation of PKA substrates was detected by western blot of HEK293 cell lysates using phospho-(Ser/Thr) PKA substrate antibody (Cell Signaling). ISO-stimulated phosphorylation of Erk1/2 was detected by western blot of HEK293 cell lysates using phospho-Thr202/Tyr204 Erk1/2 antibody (Cell Signaling).

β_2AR phosphorylation by PKA was assessed by western blot of cell lysates using phospho-Ser262/263 and phospho-Ser355/356 antisera.

β_2AR internalization—Removal of β_2AR from the cell surface upon stimulation was measured using flow cytometry according to a published protocol (Barak et al., 1994). Briefly, serum-starved cells were stimulated with agonist or inhibitors as indicated in specific figures, and cells moved to ice. Cells were fixed in 4% paraformaldehyde without permeabilization, and surface β_2AR were labeled with M1 Flag antibody (Sigma) in the presence of calcium for 1h on ice, then by anti-mouse secondary antibody conjugated to AlexaFluor-648. Fixed, labeled cells were washed again prior to flow cytometry. Surface labeling is expressed as % loss compared to untreated cells, where specific labeling is gated by comparing cells lacking Flag-β_2AR to receptor-expressing cells.

β_2AR immunocytochemistry and GFP-β-Arrestin2 translocation visualization—Flag-tagged β_2AR and mutants stably expressed in HEK293 cells were detected using antibodies. Cells were grown on 4-chamber slides. After serum-starving for 4h, cells were stimulated with isoproterenol (10 μM) or ECNO (100 μM) for 10 min unless otherwise indicated, then immediately fixed in 4% paraformaldehyde. Permeabilized cells were stained for β_2AR using Flag M2 antibody and anti-mouse-Alexa-568 or anti-rabbit-Alexa-488 secondary antibodies, and imaged on a Zeiss confocal microscope. For detection of co-localization of β_2AR and GFP-β-Arrestin2, HEK293 cells were transiently co-transfected with Flag-β_2AR and GFP-β-arrestin2. Cells were serum-starved, stimulated, fixed, stained and imaged as above.

β_2AR coupling to G_s and G_i proteins—Coupling of β_2AR to G_s and G_i proteins was measured using BRET-based proximity essentially as described (Okashah et al., 2019) but in standard HEK293 cells. Briefly, β_2AR and C265S β_2AR were fused at the carboxy terminal to Rluc8. Gβ1 and Gγ2 fused to complementing halves of Venus allowing bimolecular fluorescence complementation have been described (Hollins et al., 2009; Hynes et al., 2004). To measure G_s coupling, G_s-alpha was also overexpressed, and to measure G_i coupling, G_{i1}-alpha was overexpressed, together with receptor-Rluc8 and Venus-βγ (bimolecular complemented (Venus 156–239)-Gβ1 and (Venus 1–155)-Gγ2) (Masuho et al., 2015). This overexpression overwhelms the native G protein background to give a predominant signal via the G protein of choice in proximity to the receptor (Masuho et al., 2015).

SNO production by HEK293 cells—Receptor-stimulated SNO production was measured by photolysis-chemiluminescence as described (Hausladen et al., 2007; Zhou et al., 2019). WT or mutant receptor-expressing HEK293 cells were pretreated with PTX for 18h or not as indicated, stimulated with isoproterenol (10 μM, 10 min) and harvested. Cell pellets were lysed in HEN buffer with protease inhibitors by sonication, protein determined, and SNO-protein content quantified by UV photolysis of SNO proteins and detection of the released NO by ozone chemiluminescence.

Airway resistance in vivo—Airway responsiveness to inhaled methacholine was measured as an increase in respiratory system resistance (R_{rs}) using the flexiVent small animal ventilator (SCIREQ Inc., Montreal, Canada), as previously described (Que et al., 2005; Raffay et al., 2016). Mice were anesthetized (i.p. ketamine/xylazine; Phizer, St. Joseph, MO; Lloyd Laboratories, Shenandoah, IA), placed supine on a heated surgical bed, and tracheostomized with an 18-gauge blunt-tip cannula via a midline incision. Animals were paralyzed (i.p. pancuronium bromide; Sigma) to block spontaneous breathing and ventilated at default settings: tidal volume of 10 mL/kg, a positive end expiratory pressure of 3 cm H_2O, a rate of 150 breaths/min, and an FiO_2 of 50%. Following two recruitment breaths of deep inspiration up to 30 cm H_2O for 3 seconds, increasing doses of methacholine solution (0, 3, 6, 12.5, 25, 50, 75, 100, 200 mg/mL in saline; Sigma) were aerosolized over 10 seconds using an ultrasonic nebulizer (Aeroneb, SCIREQ) diverted into the ventilator's inspiratory flow. Serial measurements of R_{rs} were calculated by a 2.5 Hz single-frequency forced oscillation maneuver (Snapshot 150) using computer software (flexiWare 5.1, Version 7.2, SCIREQ), and an average was reported for each methacholine

dose. Animals were monitored by continuous electrocardiogram; those that did not complete the full methacholine dose response due to severe bradycardia (<60 bpm), asystole, or sustained cannula blockage with excessive secretions were excluded from the analysis.

Drug treatments were as follows: L-NAME, 100 μl total volume of 100 mg/kg in PBS was injected i.p. 1h before analysis; PTX, 100 μl total volume containing ~15 μl of 200 μg/ml PTX (Sigma) (adjusted to 100 μg/kg) and ~85 μl sterile PBS was injected i.p. 18h before analysis, as described (McGraw et al., 2007).

Aorta contraction and relaxation—Thoracic aorta was dissected from wildtype and C265S mice, cut into 3 mm rings (2 per mouse), and strung on a tension hook in an organ bath system (Radnoti, Inc), essentially as described (Zhang et al., 2022). Rings were maintained at 37°C in Krebs buffer and bubbled with 20% O_2/5% CO_2/balance nitrogen. Contraction (transducer tension) was increased by treatment with 1 μM phenylephrine, and after adjusting tension to a standard 1g, relaxation was induced by treatment with increasing concentrations of ISO, as indicated in the legend.

Isoproterenol infusion in vivo—Mice were anesthetized with ketamine and xylazine (ketamine 80 mg/kg, xylazine 8 mg/kg body weight, i.p.), an abdominal mid-line incision was made to expose the inferior vena cava (IVC), and a micro-catheter was inserted. Using an infusion pump (Harvard Apparatus, Pump 11 Elite), isoproterenol (50 ng/mL) was infused for 10 min with a flow rate at 20 μL/min, and the heart was harvested immediately and snap-frozen.

Human dust mite allergen model of allergic asthma—*Dermatophagoides pteronyssinus* and *Dermatophagoides farinae* allergens (Stallergenes-Greer, Lenoir NC) were dissolved in sterile PBS at 3mg/mL. On day 0, mice were injected (i.p.) with 100 μg of one allergen (either D.p. or D.f. as indicated). Mice were anesthetized with isofluorane gas and 30 μg of the same allergen (10 μl) was instilled intranasally daily for the next 14 days (alternating nostrils each day). On day 15 there was no allergen instillation, and mouse airways were analyzed on the flexiVent as described above, prior to harvest of tissues.

RNA isolation and Realtime reverse transcription-PCR—Total RNA from lungs was isolated by using Aurum™ Total RNA Fatty and Fibrous Tissue Kit and reverse transcribed into cDNA using iScript cDNA Synthesis Kit (Bio-Rad, Hercules, CA, USA). Quantitative real-time PCR was carried out using Fast SYBR Green or TaqMan Fast Advanced Master Mix with gene-specific primers (see Supplemental Table I), and the reactions were performed using the StepOnePlus Real-Time PCR System (Applied Biosystems Inc., Foster City, CA, USA). Endogenous beta-actin (Actb) was used to normalize gene expression. Relative mRNA expression levels (fold changes) between groups were calculated using the $\Delta\Delta C_t$ method.

Bronchoalveolar Lavage Fluid (BALF) collection and assay—After terminal anesthesia by ketamine/xylazine overdose, animals were tracheostomized and two aliquots of 1mL PBS/EDTA were instilled into the lungs with a 10 second dwell time. BALF was collected and the volume retrieved was noted, as previously described (Auten et al., 2007).

Cells in BALF were isolated by centrifugation at 1000 g for 10 minutes and re-suspended in ice-cold PBS for inflammatory cell differential counts. BALF with gross hemorrhage or with retrieval of less than 70% of instillate volume was excluded from the analysis. Immune cell types were counted using the HEMAVET 950FS (Drew Scientific) using the manufacturer's protocol.

Histology and immunohistochemistry—As previously described (Raffay et al., 2016), after terminal anesthesia by ketamine/xylazine overdose, animals were perfused *in-situ* by right ventricular puncture with PBS (pH 7.4) then 10% formalin, cannulated by tracheostomy and lungs inflation-fixed with 10% formalin at 25 cm H_2O. The trachea was ligated and the lungs were post-fixed in 10% formalin at 4° C for >24 hours. Tissue was paraffin embedded and 5 μm lung sections were processed for histology or immunostaining. Hematoxylin/Eosin and Masson's Trichrome staining were performed by the CWRU Tissue Resource Core. Immunofluorescent tissue visualization for EpCAM and MPO by confocal microscopy was performed essentially as previously described (Johnson et al., 2015, 2018). Tissue slices on slides were deparaffinized and rehydrated prior to antigen retrieval in boiling citrate. Slides were blocked with serum and incubated overnight. Slides were washed and incubated with AlexaFluor 488-conjugated rat anti-mouse EpCAM (BioLegend) and rabbit anti-mouse MPO (Abcam) antibodies. Slides were then washed and stained with AlexaFluor 647-conjugated goat anti-rabbit IgG secondary antibody (Abcam). Slides were imaged on a Leica SP5 Scanning Confocal Microscope.

Quantification and statistical analysis—Statistical analysis was performed using Graphpad Prism v8. Specific tests used, number of independent samples or replicates, and significance of results are indicated in figure legends, and all quantitative data are plotted as mean ± SD. Significance level was set at $p < 0.05$. All data are available in the figures; no large datasets or executable codesets were generated in this project.

Supplementary Material

Refer to Web version on PubMed Central for supplementary material.

Acknowledgements

The authors thank Puneet Seth for technical assistance, and Robert Lefkowitz and Howard Rockman (Duke University) and Walter Koch (Temple University) for helpful discussions.

Funded by NIH grants P01 HL075443, P01 HL128192, P01 HL158507, R01 HL126900, and R01 DK119506

Data and Materials Availability:

All data is available in the main text, Supplemental Materials or Mendeley Data. Requests for research materials should be addressed to JSS, jss156@case.edu

References

Abi-Gerges N, Szabo G, Otero AS, Fischmeister R, and Mery PF (2002). NO donors potentiate the beta-adrenergic stimulation of I(Ca,L) and the muscarinic activation of I(K,ACh) in rat cardiac myocytes. J Physiol 540, 411–424. [PubMed: 11956332]

Adachi N, Hess DT, McLaughlin P, and Stamler JS (2016). S-Palmitoylation of a Novel Site in the beta2-Adrenergic Receptor Associated with a Novel Intracellular Itinerary. J Biol Chem 291, 20232–20246. [PubMed: 27481942]

Adam L, Bouvier M, and Jones TL (1999). Nitric oxide modulates beta(2)-adrenergic receptor palmitoylation and signaling. J Biol Chem 274, 26337–26343. [PubMed: 10473590]

Amrani Y, and Bradding P (2017). beta2-Adrenoceptor Function in Asthma. Adv Immunol 136, 1–28. [PubMed: 28950943]

Antosova M, Mokra D, Pepucha L, Plevkova J, Buday T, Sterusky M, and Bencova A (2017). Physiology of nitric oxide in the respiratory system. Physiol Res 66, S159–S172. [PubMed: 28937232]

Auten RL, Mason SN, Whorton MH, Lampe WR, Foster WM, Goldberg RN, Li B, Stamler JS, and Auten KM (2007). Inhaled ethyl nitrite prevents hyperoxia-impaired postnatal alveolar development in newborn rats. Am J Respir Crit Care Med 176, 291–299. [PubMed: 17478622]

Barak LS, Tiberi M, Freedman NJ, Kwatra MM, Lefkowitz RJ, and Caron MG (1994). A highly conserved tyrosine residue in G protein-coupled receptors is required for agonist-mediated beta 2-adrenergic receptor sequestration. J Biol Chem 269, 2790–2795. [PubMed: 7507928]

Burgoyne JR, and Eaton P (2009). Transnitrosylating nitric oxide species directly activate type I protein kinase A, providing a novel adenylate cyclase-independent cross-talk to beta-adrenergic-like signaling. J Biol Chem 284, 29260–29268. [PubMed: 19726669]

Choudhry S, Que LG, Yang Z, Liu L, Eng C, Kim SO, Kumar G, Thyne S, Chapela R, Rodriguez-Santana JR, et al. (2010). GSNO reductase and beta2-adrenergic receptor gene-gene interaction: bronchodilator responsiveness to albuterol. Pharmacogenet Genomics 20, 351–358. [PubMed: 20335826]

Daaka Y, Luttrell LM, and Lefkowitz RJ (1997). Switching of the coupling of the beta2-adrenergic receptor to different G proteins by protein kinase A. Nature 390, 88–91. [PubMed: 9363896]

Fan F, Binkowski BF, Butler BL, Stecha PF, Lewis MK, and Wood KV (2008). Novel genetically encoded biosensors using firefly luciferase. ACS Chem Biol 3, 346–351. [PubMed: 18570354]

Ferguson SS, Downey WE 3rd, Colapietro AM, Barak LS, Menard L, and Caron MG (1996). Role of beta-arrestin in mediating agonist-promoted G protein-coupled receptor internalization. Science 271, 363–366. [PubMed: 8553074]

Figueroa XF, Poblete I, Fernandez R, Pedemonte C, Cortes V, and Huidobro-Toro JP (2009). NO production and eNOS phosphorylation induced by epinephrine through the activation of beta-adrenoceptors. Am J Physiol Heart Circ Physiol 297, H134–143. [PubMed: 19429833]

Forrester MT, Thompson JW, Foster MW, Nogueira L, Moseley MA, and Stamler JS (2009). Proteomic analysis of S-nitrosylation and denitrosylation by resin-assisted capture. Nat Biotechnol 27, 557–559. [PubMed: 19483679]

Foster MW, and Stamler JS (2004). New insights into protein S-nitrosylation. Mitochondria as a model system. J Biol Chem 279, 25891–25897. [PubMed: 15069080]

Friedman J, Babu B, and Clark RB (2002). Beta(2)-adrenergic receptor lacking the cyclic AMP-dependent protein kinase consensus sites fully activates extracellular signal-regulated kinase 1/2 in human embryonic kidney 293 cells: lack of evidence for G(s)/G(i) switching. Mol Pharmacol 62, 1094–1102. [PubMed: 12391272]

Gaston B, Drazen JM, Jansen A, Sugarbaker DA, Loscalzo J, Richards W, and Stamler JS (1994). Relaxation of human bronchial smooth muscle by S-nitrosothiols in vitro. J Pharmacol Exp Ther 268, 978–984. [PubMed: 7906736]

Gaston B, Reilly J, Drazen JM, Fackler J, Ramdev P, Arnelle D, Mullins ME, Sugarbaker DJ, Chee C, Singel DJ, et al. (1993). Endogenous nitrogen oxides and bronchodilator S-nitrosothiols in human airways. Proc Natl Acad Sci U S A 90, 10957–10961. [PubMed: 8248198]

Gether U, Ballesteros JA, Seifert R, Sanders-Bush E, Weinstein H, and Kobilka BK (1997a). Structural instability of a constitutively active G protein-coupled receptor. Agonist-independent activation due to conformational flexibility. J Biol Chem 272, 2587–2590. [PubMed: 9006889]

Gether U, Lin S, Ghanouni P, Ballesteros JA, Weinstein H, and Kobilka BK (1997b). Agonists induce conformational changes in transmembrane domains III and VI of the beta2 adrenoceptor. EMBO J 16, 6737–6747. [PubMed: 9362488]

Gupta MK, Asosingh K, Aronica M, Comhair S, Cao G, Erzurum S, Panettieri RA Jr., and Naga Prasad SV (2015). Defective Resensitization in Human Airway Smooth Muscle Cells Evokes β-Adrenergic Receptor Dysfunction in Severe Asthma. PLOS ONE 10, e0125803. [PubMed: 26023787]

Hausdorff WP, Bouvier M, O'Dowd BF, Irons GP, Caron MG, and Lefkowitz RJ (1989). Phosphorylation sites on two domains of the beta 2-adrenergic receptor are involved in distinct pathways of receptor desensitization. J Biol Chem 264, 12657–12665. [PubMed: 2545714]

Hausladen A, Rafikov R, Angelo M, Singel DJ, Nudler E, and Stamler JS (2007). Assessment of nitric oxide signals by triiodide chemiluminescence. Proc Natl Acad Sci U S A 104, 2157–2162. [PubMed: 17287342]

Hayashi H, Hess DT, Zhang R, Sugi K, Gao H, Tan BL, Bowles DE, Milano CA, Jain MK, Koch WJ, et al. (2018). S-Nitrosylation of beta-Arrestins Biases Receptor Signaling and Confers Ligand Independence. Mol Cell 70, 473–487 e476. [PubMed: 29727618]

Hess DT, Matsumoto A, Kim SO, Marshall HE, and Stamler JS (2005). Protein S-nitrosylation: purview and parameters. Nat Rev Mol Cell Biol 6, 150–166. [PubMed: 15688001]

Hollins B, Kuravi S, Digby GJ, and Lambert NA (2009). The c-terminus of GRK3 indicates rapid dissociation of G protein heterotrimers. Cell Signal 21, 1015–1021. [PubMed: 19258039]

Hoyte FCL, Gross LM, and Katial RK (2018). Exhaled Nitric Oxide: An Update. Immunol Allergy Clin North Am 38, 573–585. [PubMed: 30342580]

Hynes TR, Tang L, Mervine SM, Sabo JL, Yost EA, Devreotes PN, and Berlot CH (2004). Visualization of G protein betagamma dimers using bimolecular fluorescence complementation demonstrates roles for both beta and gamma in subcellular targeting. J Biol Chem 279, 30279–30286. [PubMed: 15136579]

Irannejad R, Tomshine JC, Tomshine JR, Chevalier M, Mahoney JP, Steyaert J, Rasmussen SGF, Sunahara RK, El-Samad H, Huang B, et al. (2013). Conformational biosensors reveal GPCR signalling from endosomes. Nature 495, 534–538. [PubMed: 23515162]

Jia J, Arif A, Terenzi F, Willard B, Plow EF, Hazen SL, and Fox PL (2014). Target-selective protein S-nitrosylation by sequence motif recognition. Cell 159, 623–634. [PubMed: 25417112]

Jiang LI, Collins J, Davis R, Lin KM, DeCamp D, Roach T, Hsueh R, Rebres RA, Ross EM, Taussig R, et al. (2007). Use of a cAMP BRET sensor to characterize a novel regulation of cAMP by the sphingosine 1-phosphate/G(13) pathway. Journal of Biological Chemistry 282, 10576–10584. [PubMed: 17283075]

Johnson JL, Jones MB, and Cobb BA (2015). Bacterial capsular polysaccharide prevents the onset of asthma through T-cell activation. Glycobiology 25, 368–375. [PubMed: 25347992]

Johnson JL, Jones MB, and Cobb BA (2018). Polysaccharide-experienced effector T cells induce IL-10 in FoxP3+ regulatory T cells to prevent pulmonary inflammation. Glycobiology 28, 50–58. [PubMed: 29087497]

Kersten ET, Koppelman GH, and Thio BJ (2017). Concerns with beta2-agonists in pediatric asthma - a clinical perspective. Paediatr Respir Rev 21, 80–85. [PubMed: 27515731]

Kharitonov SA, Yates D, Robbins RA, Logan-Sinclair R, Shinebourne EA, and Barnes PJ (1994). Increased nitric oxide in exhaled air of asthmatic patients. Lancet 343, 133–135. [PubMed: 7904001]

Knight JM, Mak G, Shaw J, Porter P, McDermott C, Roberts L, You R, Yuan X, Millien VO, Qian Y, et al. (2015). Long-Acting Beta Agonists Enhance Allergic Airway Disease. PLoS One 10, e0142212. [PubMed: 26605551]

Kobilka BK (2002). Agonist-induced conformational changes in the beta2 adrenergic receptor. J Pept Res 60, 317–321. [PubMed: 12464109]

Kohout TA, Lin FS, Perry SJ, Conner DA, and Lefkowitz RJ (2001). beta-Arrestin 1 and 2 differentially regulate heptahelical receptor signaling and trafficking. Proc Natl Acad Sci U S A 98, 1601–1606. [PubMed: 11171997]

Landgraf RG, Russo M, and Jancar S (2005). Acute inhibition of inducible nitric oxide synthase but not its absence suppresses asthma-like responses. European Journal of Pharmacology 518, 212–220. [PubMed: 16023634]

Laporte SA, Oakley RH, Zhang J, Holt JA, Ferguson SS, Caron MG, and Barak LS (1999). The beta2-adrenergic receptor/betaarrestin complex recruits the clathrin adaptor AP-2 during endocytosis. Proc Natl Acad Sci U S A 96, 3712–3717. [PubMed: 10097102]

Lefkowitz RJ, Pierce KL, and Luttrell LM (2002). Dancing with different partners: protein kinase a phosphorylation of seven membrane-spanning receptors regulates their G protein-coupling specificity. Mol Pharmacol 62, 971–974. [PubMed: 12391258]

Lin R, Degan S, Theriot BS, Fischer BM, Strachan RT, Liang J, Pierce RA, Sunday ME, Noble PW, Kraft M, et al. (2012). Chronic treatment in vivo with beta-adrenoceptor agonists induces dysfunction of airway beta(2) -adrenoceptors and exacerbates lung inflammation in mice. Br J Pharmacol 165, 2365–2377. [PubMed: 22013997]

Masuho I, Ostrovskaya O, Kramer GM, Jones CD, Xie K, and Martemyanov KA (2015). Distinct profiles of functional discrimination among G proteins determine the actions of G protein-coupled receptors. Sci Signal 8, ra123. [PubMed: 26628681]

Matera MG, Page CP, Calzetta L, Rogliani P, and Cazzola M (2020). Pharmacology and Therapeutics of Bronchodilators Revisited. Pharmacological Reviews 72, 218. [PubMed: 31848208]

Mathrani VC, Kenyon NJ, Zeki A, and Last JA (2007). Mouse models of asthma: can they give us mechanistic insights into the role of nitric oxide? Curr Med Chem 14, 2204–2213. [PubMed: 17691958]

McGraw DW, Elwing JM, Fogel KM, Wang WC, Glinka CB, Mihlbachler KA, Rothenberg ME, and Liggett SB (2007). Crosstalk between Gi and Gq/Gs pathways in airway smooth muscle regulates bronchial contractility and relaxation. J Clin Invest 117, 1391–1398. [PubMed: 17415415]

Moore PE, Ryckman KK, Williams SM, Patel N, Summar ML, and Sheller JR (2009). Genetic variants of GSNOR and ADRB2 influence response to albuterol in African-American children with severe asthma. Pediatr Pulmonol 44, 649–654. [PubMed: 19514054]

Nakamura T, Oh CK, Liao L, Zhang X, Lopez KM, Gibbs D, Deal AK, Scott HR, Spencer B, Masliah E, et al. (2021). Noncanonical transnitrosylation network contributes to synapse loss in Alzheimer's disease. Science 371.

Nguyen LP, Al-Sawalha NA, Parra S, Pokkunuri I, Omoluabi O, Okulate AA, Windham Li E, Hazen M, Gonzalez-Granado JM, Daly CJ, et al. (2017). beta2-Adrenoceptor signaling in airway epithelial cells promotes eosinophilic inflammation, mucous metaplasia, and airway contractility. Proc Natl Acad Sci U S A 114, E9163–E9171. [PubMed: 29073113]

Nguyen LP, Lin R, Parra S, Omoluabi O, Hanania NA, Tuvim MJ, Knoll BJ, Dickey BF, and Bond RA (2009). Beta2-adrenoceptor signaling is required for the development of an asthma phenotype in a murine model. Proc Natl Acad Sci U S A 106, 2435–2440. [PubMed: 19171883]

Nishiyama K, Nishimura A, Shimoda K, Tanaka T, Kato Y, Shibata T, Tanaka H, Kurose H, Azuma Y-T, Ihara H, et al. (2022). Redox-dependent internalization of the purinergic P2Y6 receptor limits colitis progression. Science Signaling 15, eabj0644. [PubMed: 35015570]

O'Dowd BF, Hnatowich M, Caron MG, Lefkowitz RJ, and Bouvier M (1989). Palmitoylation of the human beta 2-adrenergic receptor. Mutation of Cys341 in the carboxyl tail leads to an uncoupled nonpalmitoylated form of the receptor. J Biol Chem 264, 7564–7569. [PubMed: 2540197]

Okashah N, Wan Q, Ghosh S, Sandhu M, Inoue A, Vaidehi N, and Lambert NA (2019). Variable G protein determinants of GPCR coupling selectivity. Proc Natl Acad Sci U S A 116, 12054–12059. [PubMed: 31142646]

Ostrom RS, and Insel PA (2004). The evolving role of lipid rafts and caveolae in G protein-coupled receptor signaling: implications for molecular pharmacology. Br J Pharmacol 143, 235–245. [PubMed: 15289291]

Ozawa K, Whalen EJ, Nelson CD, Mu Y, Hess DT, Lefkowitz RJ, and Stamler JS (2008). S-nitrosylation of beta-arrestin regulates beta-adrenergic receptor trafficking. Mol Cell 31, 395–405. [PubMed: 18691971]

Papi A, Brightling C, Pedersen SE, and Reddel HK (2018). Asthma. The Lancet 391, 783–800.

Que LG, Liu L, Yan Y, Whitehead GS, Gavett SH, Schwartz DA, and Stamler JS (2005). Protection from experimental asthma by an endogenous bronchodilator. Science 308, 1618–1621. [PubMed: 15919956]

Queen LR, and Ferro A (2006). Beta-adrenergic receptors and nitric oxide generation in the cardiovascular system. Cell Mol Life Sci 63, 1070–1083. [PubMed: 16568246]

Raffay TM, Dylag AM, Di Fiore JM, Smith LA, Einisman HJ, Li Y, Lakner MM, Khalil AM, MacFarlane PM, Martin RJ, et al. (2016). S-Nitrosoglutathione Attenuates Airway Hyperresponsiveness in Murine Bronchopulmonary Dysplasia. Mol Pharmacol 90, 418–426. [PubMed: 27484068]

Rapacciuolo A, Suvarna S, Barki-Harrington L, Luttrell LM, Cong M, Lefkowitz RJ, and Rockman HA (2003). Protein kinase A and G protein-coupled receptor kinase phosphorylation mediates beta-1 adrenergic receptor endocytosis through different pathways. J Biol Chem 278, 35403–35411. [PubMed: 12821660]

Schwencke C, Okumura S, Yamamoto M, Geng YJ, and Ishikawa Y (1999). Colocalization of beta-adrenergic receptors and caveolin within the plasma membrane. J Cell Biochem 75, 64–72. [PubMed: 10462705]

Seibold A, January BG, Friedman J, Hipkin RW, and Clark RB (1998). Desensitization of beta2-adrenergic receptors with mutations of the proposed G protein-coupled receptor kinase phosphorylation sites. J Biol Chem 273, 7637–7642. [PubMed: 9516468]

Seth D, Hess DT, Hausladen A, Wang L, Wang YJ, and Stamler JS (2018). A Multiplex Enzymatic Machinery for Cellular Protein S-nitrosylation. Mol Cell 69, 451–464 e456. [PubMed: 29358078]

Shaul PW, Smart EJ, Robinson LJ, German Z, Yuhanna IS, Ying Y, Anderson RG, and Michel T (1996). Acylation targets emdothelial nitric-oxide synthase to plasmalemmal caveolae. J Biol Chem 271, 6518–6522. [PubMed: 8626455]

Stomberski CT, Hess DT, and Stamler JS (2019). Protein S-Nitrosylation: Determinants of Specificity and Enzymatic Regulation of S-Nitrosothiol-Based Signaling. Antioxid Redox Signal 30, 1331–1351. [PubMed: 29130312]

Thanawala VJ, Forkuo GS, Al-Sawalha N, Azzegagh Z, Nguyen LP, Eriksen JL, Tuvim MJ, Lowder TW, Dickey BF, Knoll BJ, et al. (2013). beta2-Adrenoceptor agonists are required for development of the asthma phenotype in a murine model. Am J Respir Cell Mol Biol 48, 220–229. [PubMed: 23204390]

Thanawala VJ, Valdez DJ, Joshi R, Forkuo GS, Parra S, Knoll BJ, Bouvier M, Leff P, and Bond RA (2015). beta-Blockers have differential effects on the murine asthma phenotype. Br J Pharmacol 172, 4833–4846. [PubMed: 26211486]

Vitale C, Maglio A, Pelaia C, and Vatrella A (2017). Long-term treatment in pediatric asthma: an update on chemical pharmacotherapy. Expert Opin Pharmacother 18, 667–676. [PubMed: 28387160]

Wanschel AC, Caceres VM, Moretti AI, Bruni-Cardoso A, de Carvalho HF, de Souza HP, Laurindo FR, Spadari RC, and Krieger MH (2014). Cardioprotective mechanism of S-nitroso-N-acetylcysteine via S-nitrosated betadrenoceptor-2 in the LDLr−/− mice. Nitric Oxide 36, 58–66. [PubMed: 24333561]

Wendell SG, Fan H, and Zhang C (2020). G Protein-Coupled Receptors in Asthma Therapy: Pharmacology and Drug Action. Pharmacol Rev 72, 1–49. [PubMed: 31767622]

Whalen EJ, Foster MW, Matsumoto A, Ozawa K, Violin JD, Que LG, Nelson CD, Benhar M, Keys JR, Rockman HA, et al. (2007). Regulation of beta-adrenergic receptor signaling by S-nitrosylation of G-protein-coupled receptor kinase 2. Cell 129, 511–522. [PubMed: 17482545]

Wu H, Romieu I, Sienra-Monge JJ, Estela Del Rio-Navarro B, Anderson DM, Jenchura CA, Li H, Ramirez-Aguilar M, Del Carmen Lara-Sanchez I, and London SJ (2007). Genetic variation in S-nitrosoglutathione reductase (GSNOR) and childhood asthma. J Allergy Clin Immunol 120, 322–328. [PubMed: 17543375]

Xiang Y, Rybin VO, Steinberg SF, and Kobilka B (2002). Caveolar localization dictates physiologic signaling of beta 2-adrenoceptors in neonatal cardiac myocytes. J Biol Chem 277, 34280–34286. [PubMed: 12097322]

Zhang J, Ferguson SS, Barak LS, Menard L, and Caron MG (1996). Dynamin and beta-arrestin reveal distinct mechanisms for G protein-coupled receptor internalization. J Biol Chem 271, 18302–18305. [PubMed: 8702465]

Zhang R, Hausladen A, Qian Z, Liao X, Premont RT, and Stamler JS (2022). Hypoxic vasodilatory defect and pulmonary hypertension in mice lacking hemoglobin beta-cysteine93 S-nitrosylation. JCI Insight 7.

Zhou HL, Zhang R, Anand P, Stomberski CT, Qian Z, Hausladen A, Wang L, Rhee EP, Parikh SM, Karumanchi SA, et al. (2019). Metabolic reprogramming by the S-nitroso-CoA reductase system protects against kidney injury. Nature 565, 96–100. [PubMed: 30487609]

Highlights

- β_2AR is S-nitrosylated at Cys265, mediating receptor desensitization
- S-nitrosylation drives β_2AR internalization via caveolae
- β_2AR lacking S-nitrosylation exhibits prolonged signaling to cAMP, Erk and NO
- Mice with β_2AR refractory to S-nitrosylation are protected from asthma

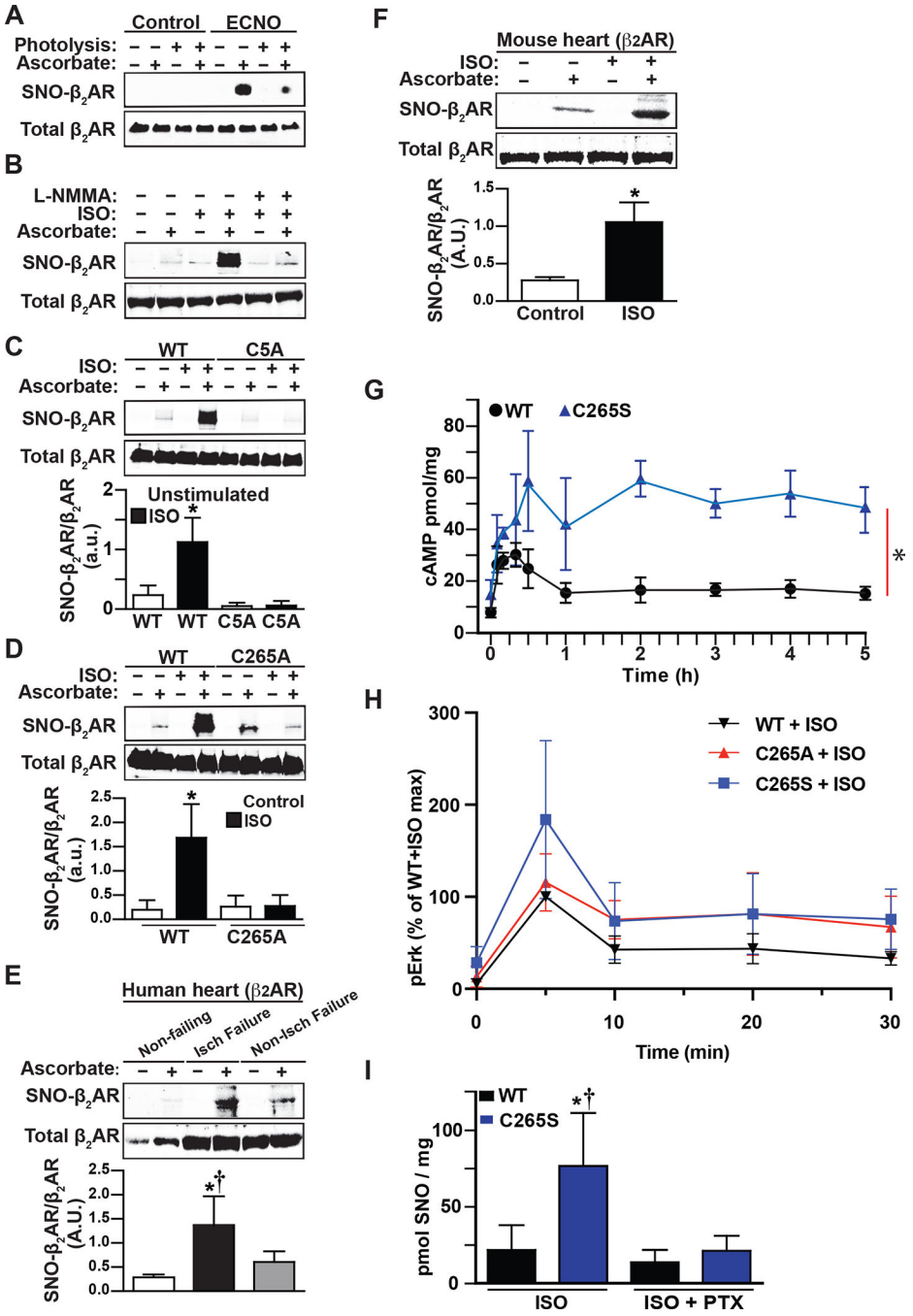

Figure 1. β_2AR is S-nitrosylated primarily at Cys265 in response to NO donor or activation by agonist to regulate receptor desensitization.

A. SNO-β_2AR is detected by immunoblotting with anti-Flag antibody after isolation of SNO-proteins (by SNO-RAC) from HEK293 W9 cells stably expressing Flag-β_2AR, untreated or treated with ECNO (100 μM, 10 min) prior to harvesting cells. Ascorbate (−) and UV photolysis during Cys blocking, which removes SNO from Cys residues, serve as specificity controls. Total β_2AR control is from Flag immunoblot of lysate. Blot is representative of 3 replicates. B. SNO-β_2AR detected by SNO-RAC of lysates from HEK293 cells stably expressing Flag-β_2AR, untreated or treated with isoproterenol (ISO,

10 μM, 10 min). The NOS inhibitor L-NMMA was incubated with cells for 2h prior to stimulation. Total β_2AR control is from Flag immunoblot of lysate. Blot is representative of 5 replicates. C. SNO-β_2AR detected by SNO-RAC of lysates from HEK293 cells stably expressing Flag-β_2AR WT (W9) or Flag-β_2AR 5-Cys mutant (C5A), untreated or treated with ISO (10 μM, 10 min) prior to harvesting cells. Total β_2AR control is from Flag immunoblot of lysate. Blot shown is representative of 5 replicates, which were quantified by densitometry and graphed as mean±SD. $p<0.0001$ by one-way ANOVA for treatment ($F(3,16) = 29.22$); * $p<0.0001$ basal vs ISO by Tukey test. D. SNO-β_2AR detected by SNO-RAC of lysates from HEK293 cells stably expressing Flag-β_2AR WT (W9) or Flag-β_2AR C265A mutant, untreated or treated with isoproterenol (ISO, 10 μM, 10 min) prior to harvesting cells. Total β_2AR control is from Flag immunoblot of lysate. Blot is representative of 6 replicates. $p<0.0001$ by one-way ANOVA for treatment ($F(3,20) = 22.09$); * $p<0.0001$ basal vs ISO by post-hoc Tukey multiple comparisons test. E. SNO-β_2AR detected by SNO-RAC of lysates from human heart samples, from normal non-failing heart, ischemic failing heart, and non-ischemic failing heart. Total β_2AR control is from anti-β_2AR immunoblot of lysate. Representative blot is shown, of 3 non-failing, 3 ischemic and 3 non-ischemic failing heart samples tested, which are all quantified in the bar graph. * $p<0.05$ vs non-failing and non-ischemic failing heart by one-way ANOVA with Tukey post-hoc test. F. SNO-β_2AR detected by SNO-RAC of lysates from mouse heart after 10 min i.v. infusion of saline control or isoproterenol (ISO). Total β_2AR control is from anti-β_2AR immunoblot of lysate. Blot shown is representative of 3 replicates, which are all quantified in the bar graph. * $p<0.05$ by t-test. G. Time course of ISO (10 μM)-stimulated cAMP accumulation in HEK293 cells stably expressing WT Flag-β_2AR (W9) or Flag-β_2AR-C265S mutation for the indicated times, measured using ELISA assay from cell lysates. Data are shown as mean±SD for 3 assays. * $p=0.0033$ in RM-ANOVA by genotype ($F(1, 4) = 39.5$). H. Time course of ISO (10 μM)-stimulated Erk activation in HEK293 cells stably expressing Flag-β_2AR WT (W9) or Flag-β_2AR-C265S or C265A mutations for the indicated times, measured using immunoblotting for phospho-Thr202/Tyr204-Erk1/2 from cell lysates, normalized to total Erk. Cells were preincubated with 100 ng/ml PTX overnight, or untreated. Data are plotted as mean±SD for 4 assays; representative pErk/Erk blots are shown as Supplemental Fig 2E and PTX sensitivity is plotted in Supplemental Fig 2F. I. Total protein SNO levels in HEK293 cells expressing WT or β_2AR C265S, pretreated with PTX (100 ng/ml for 16h) and stimulated with ISO (10 μM for 5 min), measured by Hg-coupled photolysis/chemiluminescence. Data are shown as mean±SD for 5 assays; representative Nitrolyte traces are shown as Supplemental Fig 2G. * $p<0.05$ vs WT, † $p<0.05$ vs C265S+PTX using one-way ANOVA ($F(3,16) = 10.34$) and post-hoc Tukey multiple comparisons test.

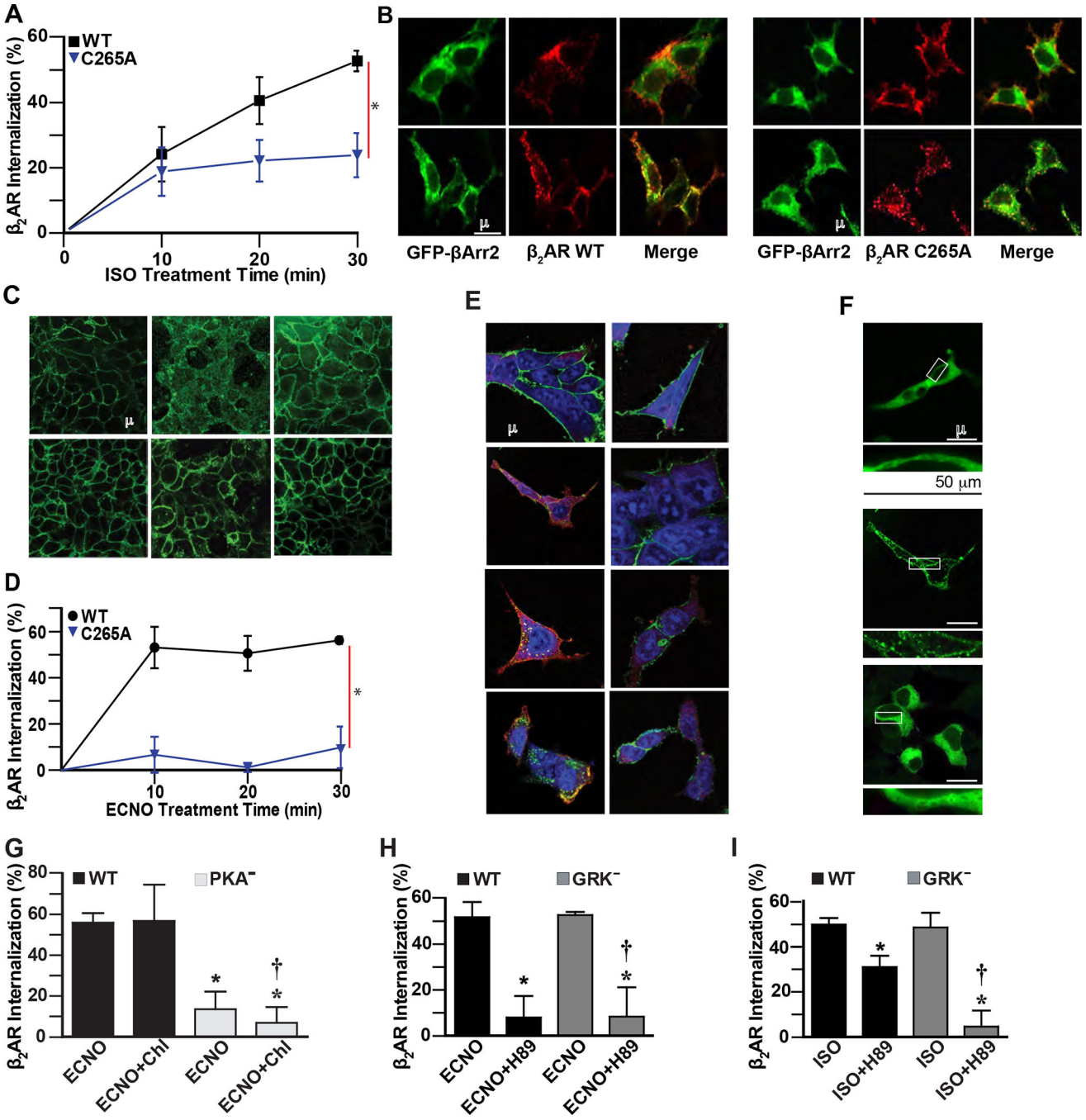

Figure 2. β_2AR S-nitrosylation drives agonist-independent receptor internalization through the caveolae pathway, but not the GRK/β-arrestin2/clathrin pathway.

A. ISO (10 μM) induces time-dependent internalization of cell surface WT Flag-β_2AR in HEK293 cells, but internalization of C265A β_2AR is reduced, quantified by flow cytometry. Data are shown as mean±SD for 9 assays. * p<0.0001 for cumulative response (area under curve) for WT vs mutant using two-tail t-test test. B. ISO (10 μM, 10 min) induces colocalization of HA-β_2AR or HA-β_2AR C265A with β-Arrestin2-GFP (green) in HEK293 cells, detected by confocal microscopy (yellow) after labeling with anti-HA antibody/anti-rabbit AlexaFluor-568 (β_2AR, red). Data are representative of 12 cells surveyed in 3

experiments. C. ECNO treatment (100 μM, 10 min) or overexpression of eNOS induces internalization of cell surface WT but not C5A mutant Flag-β_2AR in HEK293 cells, detected by confocal microscopy using labeling with anti-Flag antibody and anti-mouse AlexaFluor-488. Images are representative of 5 assays. D. ECNO (100 μM) induces time-dependent internalization of cell surface WT but not C265A Flag-β_2AR in HEK293 cells, quantified by flow cytometry after labeling with anti-Flag M1 and AlexaFluor-647. Data are shown as mean±SD for 3 assays. * $p<0.0001$ for cumulative response (area under curve) for WT vs drug-treated using two-tail t-test test. E. ISO (10 μM) treatment for the indicated times induces colocalization (yellow) of HA-β_2AR and Flag-β-Arrestin2 in HEK293 cells, while ECNO (100 μM) treatment does not, detected by confocal microscopy after labeling with anti-HA antibody/anti-rabbit AlexaFluor-488 (β_2AR, green), anti-Flag antibody/anti-goat AlexaFluor-568 (β-Arrestin2, red), and Draq5 (nuclei, blue). Data are representative of 15 cells surveyed in 3 experiments. F. ISO (10 μM, 10 min) induces translocation of β-Arrestin2-GFP (green) in HEK293 cells expressing WT β_2AR, but treatment with ECNO (50 μM, 20 min) does not, detected by confocal microscopy. Lower panels are magnified versions of the boxed regions. Data are representative of 15 cells surveyed in 3 experiments. G. ECNO-driven (50 μM, 20 min) internalization of WT β_2AR is not inhibited by the clathrin inhibitor chlorpromazine (Chl, 10 μM 1h), while the β_2AR deficient in PKA phosphorylation sites (PKA^-) is not internalized by ECNO, as measured by flow cytometry. Data are shown as mean±SD for 3 assays in triplicate. $p<0.0001$ by one-way ANOVA for treatment ($F(3,32) = 75.29$); * $p<0.0001$ vs WT ECNO and † $p<0.0001$ vs WT ECNO Chl by Tukey test. H. ECNO-driven (50 μM, 20 min) internalization of WT β_2AR and GRK^- mutant β_2AR is inhibited by the PKA inhibitor H-89 (10 μM, 15 min prior to ECNO), as measured by flow cytometry. Data are shown as mean±SD for 6 assays. $p<0.0001$ by one-way ANOVA for treatment ($F(3,20) = 84.55$); * $p<0.0001$ vs WT ISO and † $p<0.0001$ vs GRK^- ISO by Tukey test. I. ISO-driven (10 μM, 20 min) internalization of WT β_2AR is partially inhibited by the PKA inhibitor H-89 (10 μM, 15 min prior to agonist), while internalization of GRK^- mutant β_2AR is completely inhibited, as measured by flow cytometry. Data are shown as mean±SD for 6 assays. $p<0.0001$ by one-way ANOVA for treatment ($F(3,20) = 18.62$); * $p<0.0001$ vs WT ISO and † $p<0.0001$ vs GRK^- ISO by Tukey test.

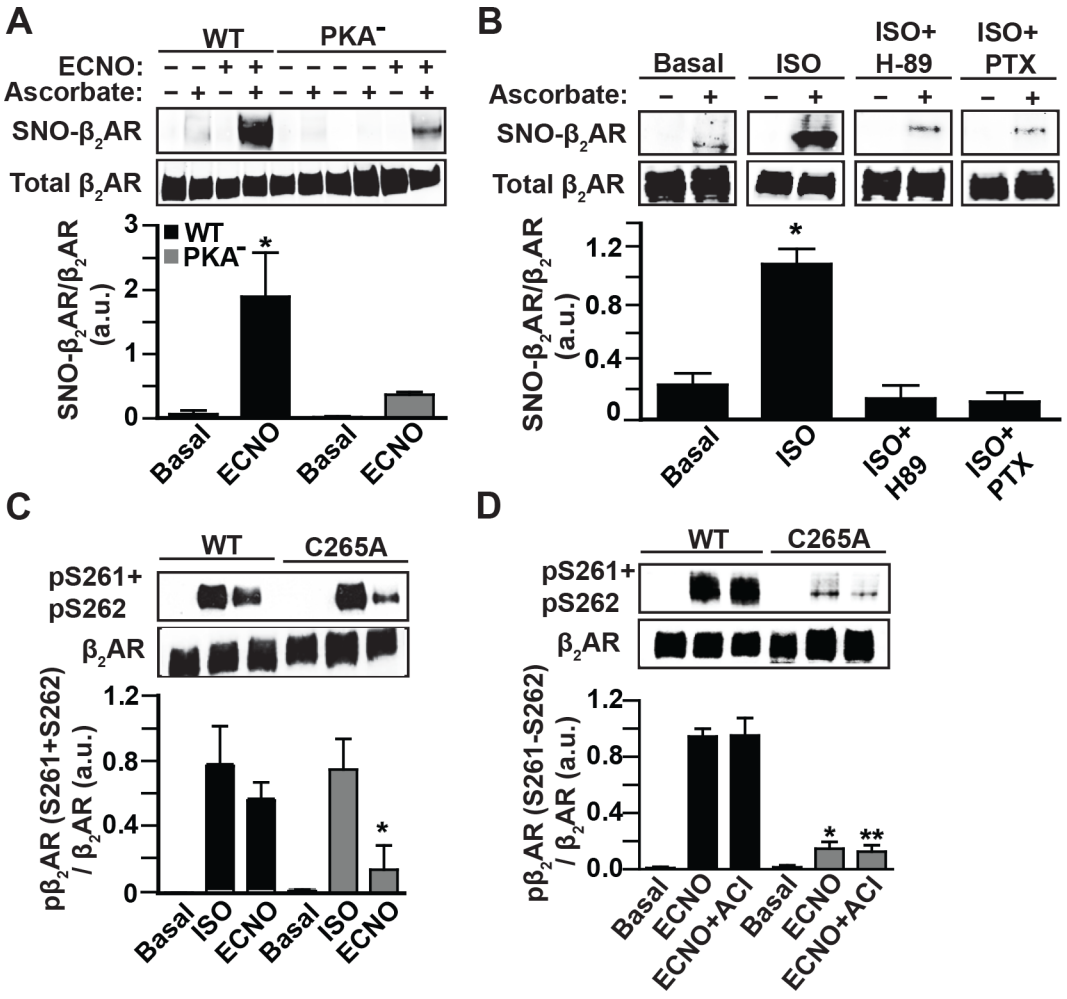

Figure 3. β_2AR S-nitrosylation and PKA phosphorylation are co-dependent.

A. SNO-β_2AR detected by SNO-RAC of lysates from HEK293 cells stably expressing Flag-β_2AR WT or Flag-β_2AR PKA$^-$ mutant, untreated or treated with ECNO (100 μM, 10 min) prior to harvesting cells. Total β_2AR control is from Flag immunoblot of lysate. Blots are representative of 4 replicates. p<0.0001 by one-way ANOVA for treatment (F (3,16) = 39.37); * p<0.0001 basal vs ECNO by Tukey test. B. SNO-β_2AR detected by SNO-RAC of HEK293 cells stably expressing Flag-β_2AR, in cells pretreated with PKA inhibitor H-89 (10 μM, 15 min prior to ISO) or the G_i inhibitor PTX (100 ng/ml, 16h), untreated or treated with ISO (10 μM, 10 min), prior to harvesting cells. Total β_2AR control is from Flag immunoblot of lysate. Blots are representative of 3 replicates that were quantified by densitometry and plotted as mean±SD. p<0.0001 by one-way ANOVA for treatment (F (3, 8) = 84.86); * p<0.0001 basal/H-89/PTX samples vs ISO by Tukey test. C. PKA phosphorylation of Flag-β_2AR WT or C265A mutant in stable HEK293 cells, stimulated with ISO (10 μM, 10 min) or ECNO (100 μM, 10 min), detected by immunoblotting of cell lysates using anti-phospho-Ser261/Ser262-β_2AR antiserum. Blots are representative of 3 replicates that were quantified by densitometry and plotted as mean±SD. p<0.0001 by one-way ANOVA for treatment F (5, 12) = 18.56; * p<0.0382 WT+ECNO vs C265A+ECNO by Tukey test. D. Protein kinase A-mediated phosphorylation of the Flag-β_2AR WT or

C265A mutant in stable HEK293 cells, pretreated with adenylyl cyclase inhibitor cocktail (membrane AC inhibitor 2',5'-dideoxyadenosine 3'-triphosphate 10 μM plus soluble AC inhibitor KH7 50 μM, preincubated 1h), stimulated with ECNO (100 μM, 10 min), detected by immunoblotting of cell lysates using anti phospho-Ser261/Ser262-β_2AR antiserum. Blot shown is representative of 3 replicates that were quantified by densitometry and plotted as mean±SD. $p<0.0001$ by one-way ANOVA for treatment ($F(5,12) = 161.9$); * $p<0.0001$ vs WT ECNO and ** $p<0.0001$ vs WT ECNO+ACI by Tukey test.

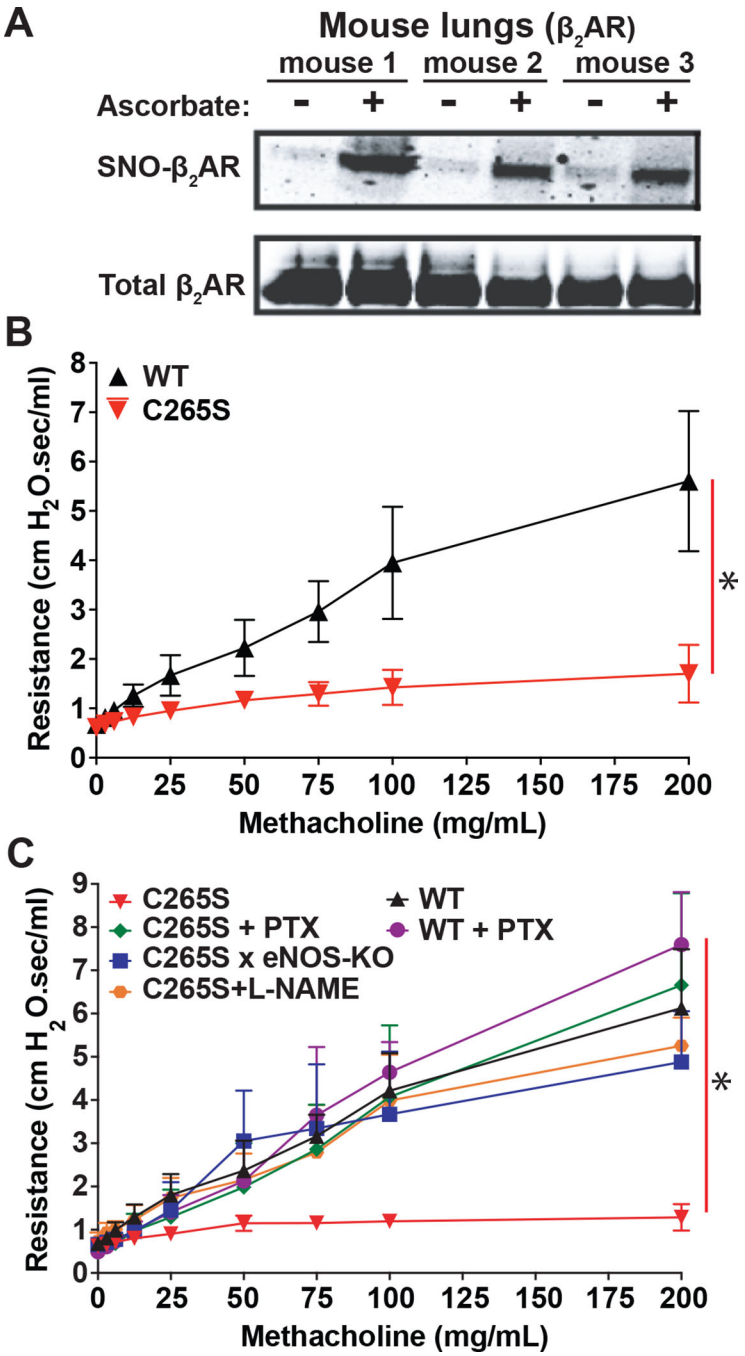

Figure 4. Essential role of endogenous NO in airway relaxation is counteracted by β_2AR S-nitrosylation.

A. Native SNO-β_2AR detected by SNO-RAC of lysates from WT mouse lung (n=3 mice). Total β_2AR control is from immunoblot of lung lysate. B. Respiratory system resistance in mice bearing WT β_2AR vs. β_2AR C265S knock-in (C265S), measured by flexiVent after the indicated progressive dose of aerosolized methacholine. Data are shown as mean±SD for 16 mice each. * p<0.0001 for cumulative response (area under curve) by genotype using two-tail t-test. C. Airway resistance in mice bearing WT β_2AR vs. β_2AR C265S knock-in (C265S), after pretreatment with PTX (100 μg/kg i.p. 18h prior to assay) or L-NAME (100

mg/kg i.p. 1h prior to assay), or in mice bred to have β_2AR C265S plus eNOS deficiency. Resistance was measured by flexiVent after the indicated dose of methacholine. Data are shown as mean±SD for 8 mice each. $p<0.0001$ in a two-way repeated measures ANOVA among genotypes and treatment over dose ($F(5, 42) = 10.37$); * $p<0.0002$ for cumulative response (area under curve) using Tukey test, for all groups vs C265S.

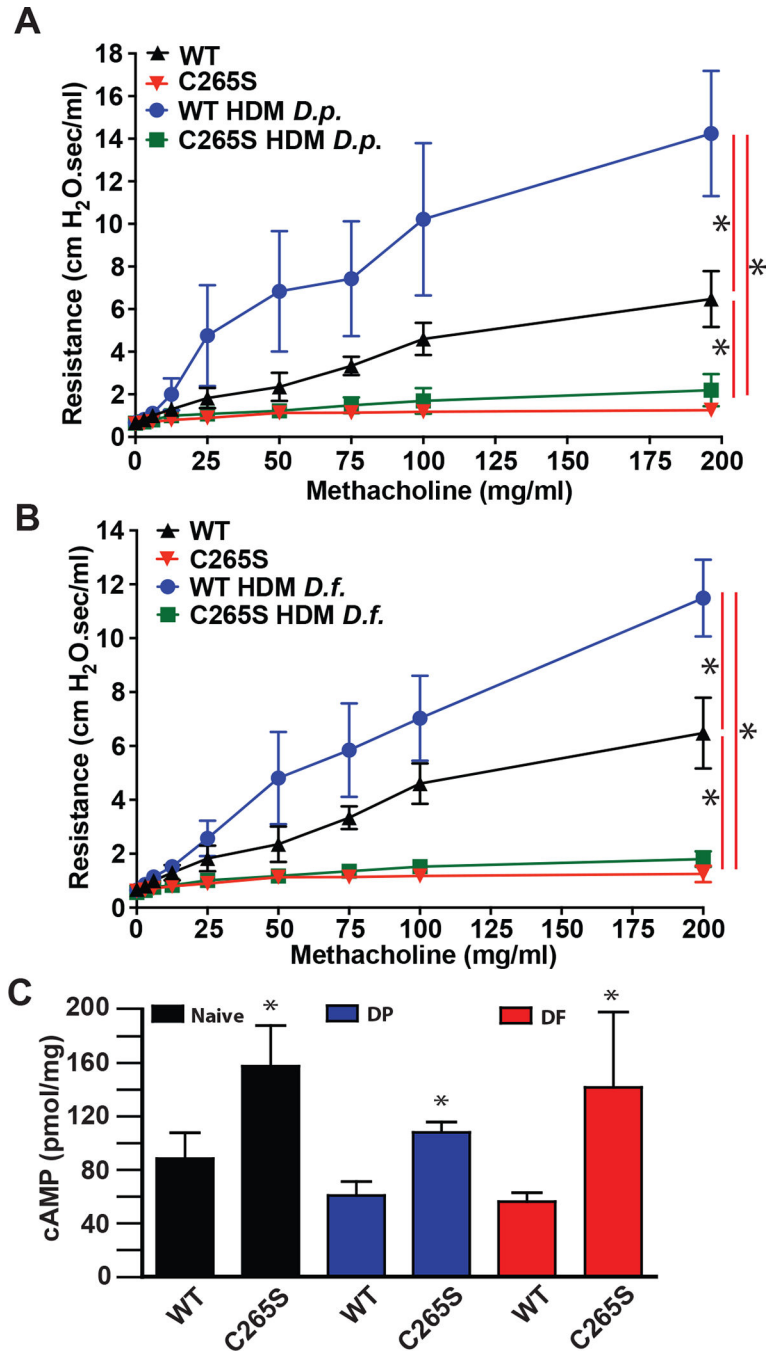

Figure 5. β_2AR C265S protects airway function in allergic asthma model.

A. Respiratory system resistance in mice bearing β_2AR WT vs. β_2AR C265S knock-in (C265S), following pretreatment with house dust mite *D. pteronyssinus* allergen (*D.p.*; 100 μg i.p. on day 0, 30 μg intranasal instillation on days 1–14, tested on day 15), measured by flexiVent after the indicated dose of aerosolized methacholine. Data are shown as mean±SD for 9 mice each. $p<0.0001$ in a two-way repeated measures ANOVA among genotypes and treatment over dose (F (3, 32) = 74.42); * $p<0.0001$ for cumulative response (area under curve) using Tukey test. B. Airway resistance in WT vs. C265S mice, following

pretreatment with house dust mite *D. farinae* allergen (*D.f.*; treatment as in (A)), measured by flexiVent after the indicated dose of aerosolized methacholine. Data are shown as mean±SD for 9 mice each. $p<0.0001$ in a two-way repeated measures ANOVA among genotypes and treatment over dose ($F(3, 32) = 156.1$); * $p<0.0001$ for cumulative response (area under curve) using Tukey test. C. Cyclic AMP levels in whole lung lysate from WT or C265S mice before vs after treatment with house dust mite allergens, measured by ELISA. Data are shown as mean±SD for 4 mice each. * $p<0.05$ using two-tailed t-test comparing WT and C265S for each treatment (naïve, D.p., D.f.).

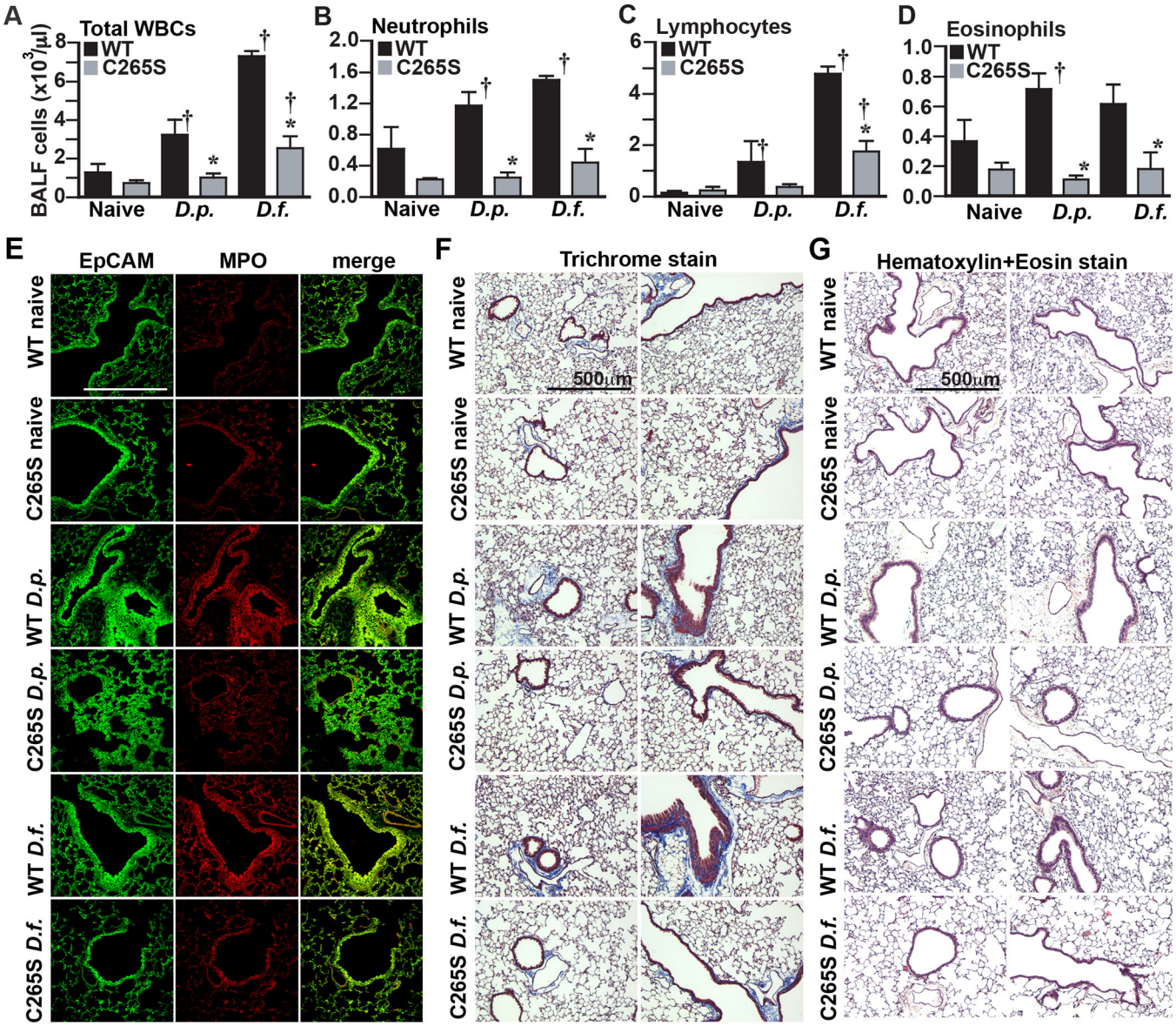

Figure 6. β_2AR C265S protects against immune, inflammatory and remodeling effects in asthma model.

A.-D. Total infiltrating immune cell numbers in bronchoalveolar lavage fluid from WT and C265S mice treated with house dust mite allergens, measured by HEMAVENT 950 cytometry. (A) Total infiltrating white blood cells (WBC), (B) neutrophils, (C) lymphocytes, (D) eosinophils. Data is shown as mean±SD from samples from 3 mice. $p<0.0001$ for all panels A-D by one-way ANOVA; * $p<0.005$ vs corresponding WT treatment control, or † $p<0.05$ from corresponding naïve control, by Tukey test. E. Immunofluorescent staining for epithelial cell adhesion molecule (EpCAM, green) and myeloperoxidase (MPO, red), and merge for colocalization (yellow), in lung sections from WT and C265S mice treated with the indicated house dust mite allergens. Immune cell infiltration at sites of hyperplasia (visible as yellow) are prominent in allergen-treated WT mice, but largely absent from C265S mice. Confocal photos shown are representative of 4 individual mice assessed

in each condition. F. Masson's Trichrome staining in sections of lungs from WT and C265S mice treated with house dust mite allergens. Bronchial muscle thickening, epithelial hyperplasia and luminal occlusion are prominent in allergen-treated WT mice, but largely absent from C265S mice. Photos shown are representative of 4 individual mice assessed in each condition. G. H&E staining in sections of lungs from WT and C265S mice treated with house dust mite allergens. Epithelial hyperplasia, immune cell infiltration and luminal occlusion are prominent in allergen-treated WT mice, but largely absent from C265S mice. Photos shown are representative of 4 individual mice assessed in each condition.

KEY RESOURCES TABLE

REAGENT or RESOURCE	SOURCE	IDENTIFIER
Antibodies		
anti-Flag M1 (mouse monoclonal)	Sigma-Aldrich	Cat# F3040 RRID:AB_439712
anti-Flag M2 (mouse monoclonal)	Sigma-Aldrich	Cat# F3165 RRID:AB_439685
anti-HA-7 (mouse monoclonal)	Sigma-Aldrich	Cat# H9658 RRID:AB_260092
anti-Erk1/2	Cell Signaling Technology	Cat# 4695 RRID:AB_390779
anti-Erk1/2 pThr202+pTyr204	Cell Signaling Technology	Cat# 9101 RRID:AB_331646
anti-Protein kinase A - catalytic subunit	Cell Signaling Technology	Cat# 5842 RRID:AB_10706172
anti-Protein kinase A - catalytic subunit, pThr197	Cell Signaling Technology	Cat# 5661 RRID:AB_10707163
anti-Pan-PKA substrate pSer/pThr	Cell Signaling Technology	Cat# 9621 RRID:AB_330304
anti-β_2 adrenergic receptor (H-20)	Santa Cruz Biotechnology	Cat# sc-569 Lot# L0415 RRID:AB_630926
anti-β_2AR pSer261/pSer262	Robert Lefkowitz (Nobles et al., 2011)	N/A
anti-β_2AR pSer345/pSer346	Robert Lefkowitz (Nobles et al., 2011)	N/A
anti-β_1AR (A-20)	Santa Cruz Biotechnology	Cat# sc-567 RRID:AB_2225390
anti-Phospholipase C-beta1 (D8)	Santa Cruz Biotechnology	Cat# sc-5291 RRID:AB_628118
anti-Phospholipase C-beta3 (D-7)	Santa Cruz Biotechnology	Cat# sc-133231 RRID:AB_2299534
anti-EpCAM (CD326) - Alexafluor488 Conjugate	BioLegend	Cat# 118210 RRID:AB_1134099
anti-myeloperoxidase	Abcam	Cat# ab45977 RRID:AB_944318
anti-GAPDH (6C5)	Millipore (Sigma-Aldrich)	Cat# MAB374 RRID:AB_2107445
Donkey anti-rabbit-Alexafluor594	Molecular Probes, ThermoFisher	Cat# A32754 RRID:AB_2762827
Goat anti-mouse-Alexafluor568	Molecular Probes, ThermoFisher	Cat# A11031 RRID:AB_144696
Goat anti-rabbit-Alexafluor488	Molecular Probes, ThermoFisher	Cat# A32731 RRID:AB_2633280
Goat anti-rabbit-Alexafluor647	Abcam	Cat# ab150083 RRID:AB_2714032
Bacterial and Virus Strains		
N/A		
Biological Samples		
Human heart failure patient ventricular tissue	Biorepository and Precision Pathology Center, Duke University	N/A
Chemicals, Peptides, and Recombinant Proteins		
Thiopropyl-Sepharose 6B	Sigma-Aldrich	T8387
S-Methyl methanethiosulfonate (MMTS)	Sigma-Aldrich	64306
L-N^G-monomethyl arginine (L-NMMA)	Cayman Chemical	80200
L-N^G-Nitroarginine methyl ester (L-NAME)	Cayman Chemical	80210

REAGENT or RESOURCE	SOURCE	IDENTIFIER
(−)-Isoproterenol (+)-bitartrate salt	Sigma-Aldrich	I2760
Salbutamol	Sigma-Aldrich	S8260
Salmeterol	Sigma-Aldrich	S5068
Pindolol	Sigma-Aldrich	P0778
Procaterol	Sigma-Aldrich	P9180
Fenoterol	Sigma-Aldrich	F1016
Epinephrine	Sigma-Aldrich	E4250
Isoetharine	Sigma-Aldrich	I3639
Pertussis toxin	Sigma-Aldrich	P7208
DRAQ5	Thermo-Fisher	62251
β-methyl cyclodextrin	Sigma-Aldrich	C4555
Chlorpromazine hydrochloride	Sigma-Aldrich	C0982
H-89 (N-[2-(p-Bromocinnamylamino)ethyl]-5-isoquinolinesulfonamide dihydrochloride)	Sigma-Aldrich	B1427
Genistein	Sigma-Aldrich	G6649
Filipin III	Sigma-Aldrich	SAE0087
Methacholine chloride	Sigma-Aldrich	1396364
2’,5’-dideoxyadenosine 3’-triphosphate	Sigma-Aldrich	D0939
KH7 ((E)-2-(1H-Benzo[d]imidazol-2-ylthio)-N’-(5-bromo-2-hydroxybenzylidene)propanehydrazide)	Sigma-Aldrich	K3394
house dust mite *Dermatophagoides pteronyssinus* allergen	Stallergenes-Greer	B70
house dust mite *Dermatophagoides farinae* allergen	Stallergenes-Greer	B64
X-tremeGENE 9 transfection reagent	Sigma-Aldrich	6365779001
X-tremeGENE HP transfection reagent	Sigma-Aldrich	6366244001
KT-5720	Tocris	1288
SQ-22536	Tocris	1435
Phenylephrine hydrochloride	Sigma-Aldrich	1533002
[^{3}H]-alprenolol; Dihydroalprenolol Hydrochloride, Levo-[Ring, Propyl-3H(N)]	PerkinElmer	NET720250UC
Critical Commercial Assays		
PARAMETER cAMP ELISA kit	R&D Systems	KGE012
GloSensor cAMP biosensor reagent	Promega	E1290
Aurum Total RNA Fatty and Fibrous Tissue Kit	Bio-Rad	7326830
iScript cDNA Synthesis Kit	Bio-Rad	1708890
Fast SYBR Green Master Mix	Thermo-Fisher	4385612
TaqMan Fast Advanced Master Mix	Thermo-Fisher	4444556
cAMP Phosphodiesterase activity kit (Fluorometric)	Biovision	K2013-100
Deposited Data		
Image raw data files	Mendeley Data	http://dx.doi.org/10.17632/p2zycrb6dr

REAGENT or RESOURCE	SOURCE	IDENTIFIER
Experimental Models: Cell Lines		
HEK293	ATCC	Cat# CRL-1573 RRID:CVCL_0045
HEK293 W9, stably expressing human Flag-β2AR	Robert Lefkowitz, Duke University	Shenoy et al., 2006 PMID 16280323
HEK293, stably expressing HA-ATR1	this study	N/A
Arrb1-/- mouse embryonic fibroblast (MEF) cell line	Robert Lefkowitz, Duke University	Kohout et al., 2001, PMID 11171997
Arrb2-/- mouse embryonic fibroblast (MEF) cell line	Robert Lefkowitz, Duke University	Kohout et al., 2001, PMID 11171997
Experimental Models: Organisms/Strains		
Mouse: Adrb2$^{Cys265Ser/Cys265Ser}$ knock-in	this study	N/A
Mouse: Nos3 knockout: B6.129P2-*Nos3*^{tm1Unc}/J	The Jackson Laboratories	Cat# Jax:002684 RRID:IMSR_JAX:002684
Mouse: FLP deleter strain: B6.Cg-Tg(ACTFLPe)9205Dym/J	The Jackson Laboratories	Cat# Jax:005703 RRID:IMSR_JAX:005703
Mouse: FVB.129-Adrb2^{tm1Bkk}/J	The Jackson Laboratories	Cat# Jax: 031496 RRID:IMSR_JAX:031496
Oligonucleotides		
See Supplemental Table I	this study	N/A
Recombinant DNA		
GloSensor-20F cAMP biosensor	Promega	E1171
CAMYEL cAMP biosensor	Paul Sternweis, UT Southwestern, Jiang et al., 2007 PMID 17283075	N/A
Flag-β_2AR (human)	Robert Lefkowitz, Oppermann et al., 1996 PMID 8755530	N/A
Flag-β_2AR (human), PKA$^-$ mutant	Robert Lefkowitz, Seibold et al., 1998 PMID 9516468	N/A
Flag-β_2AR (human), GRK$^-$ mutant	Robert Lefkowitz, Seibold et al., 1998 PMID 9516468	N/A
GFP-β-Arrestin2	Robert Lefkowitz, Barak et al, 1997 PMID 9346876	N/A
Venus 156-239-Gβ1, Venus 1-155-Gγ2	Nevin Lambert, Hollins et al., 2009 PMID 19258039	N/A
β_2AR-NanoLuc	Nevin Lambert, Okashah et al., 2019 PMID 31142646	
HA-ATR1 (human)	Robert Lefkowitz, Tohgo et al, 2002 PMID: 11777902	N/A
Software and Algorithms		
Graphpad Prism (v7, v9)	Graphpad Software	version 7, version 9

REAGENT or RESOURCE	SOURCE	IDENTIFIER
Other		
N/A		